

# FLT4 as a marker for predicting prognostic risk of refractory acute myeloid leukemia

Ji Yoon Lee,<sup>1,2</sup> Sung-Eun Lee,<sup>3</sup> A-Reum Han,<sup>1</sup> Jongeun Lee,<sup>2</sup> Young-sup Yoon<sup>2,4</sup> and Hee-Je Kim<sup>1,3</sup>

<sup>1</sup>Leukemia Research Institute, College of Medicine, the Catholic University of Korea, Seoul, Korea; <sup>2</sup>Severance Biomedical Science Institute, Yonsei University College of Medicine, Seoul, Korea; <sup>3</sup>Catholic Hematology Hospital, Seoul St. Mary's Hospital, College of Medicine, the Catholic University of Korea, Seoul, Korea and <sup>4</sup>Department of Medicine, Emory University, Atlanta, GA, USA

**Correspondence:**

Y-s. Yoon  
[yyoon5@emory.edu](mailto:yyoon5@emory.edu)

H-J. Kim  
[cumckim@catholic.ac.kr](mailto:cumckim@catholic.ac.kr)

**Received:** November 24, 2022.

**Accepted:** June 5, 2023.

**Early view:** June 15, 2023.

<https://doi.org/10.3324/haematol.2022.282472>

©2023 Ferrata Storti Foundation

Published under a CC BY-NC license



## Supplementary Information

### FLT4 as a marker for predicting prognostic risk of refractory acute myeloid leukemia

Ji Yoon Lee, Sung-Eun Lee, A-Reum Han, Jongeun Lee, Young-sup Yoon, Hee-Je Kim

#### Supplementary methods

##### Quantitative RT-PCR (qRT-PCR)

Isolation of total RNA and cDNA synthesis were performed as previously described.(1) Information on Taqman primer/probe sets (Biosearch Technologies, Novato, CA) used in this study is listed in Supplementary Table 2. Relative mRNA expression of target genes was calculated using the comparative CT method.(2) All target genes were normalized to *GAPDH* in multiplexed reactions performed in triplicate. Differences in CT values were calculated for each target mRNA by subtracting the mean value of *GAPDH* (relative expression= $2^{-\Delta CT}$ ).

##### Flow cytometry and fluorescence-activated cell sorting

FACS staining and cell isolation were performed as previously described.(3) Cells were briefly resuspended in 100  $\mu$ l of rinsing buffer and incubated with antibodies. After washing, the cells were analyzed using a FACSCalibur flow cytometer equipped with Cell Quest software (BD Biosciences, San Diego, CA, USA). We used phycoerythrin (PE)-conjugated mouse anti-human CD34 (555822, BD Pharmingen), PE-Cy<sup>TM</sup>5-conjugated mouse anti-human CD38 (555461, BD Pharmingen) and mouse anti-human VEGFR-3 (MAB3757; Millipore, Billerica, MA, USA) as primary antibodies to examine cells. For engraftment studies, FITC-conjugated mouse anti-human CD45 (555482, BD Pharmingen), allophycocyanin (APC)-conjugated rat anti-mouse

CD45 (559864, BD Pharmingen) and FITC-conjugated anti-human CD7 (347480, BD Biosciences) were used. For secondary antibodies, proper isotype-matched IgG and unstained controls were used; in the case of internalization studies, PE-conjugated anti-mouse IgG2b $\kappa$  (559529, BD Pharmingen) and FITC-conjugated anti-mouse IgG2a (sc-2079, Santa Cruz) were used. The CD34<sup>+</sup>CD38<sup>-</sup> cells were isolated with FACSmoflo (Beckman Coulter MoFlo, USA).

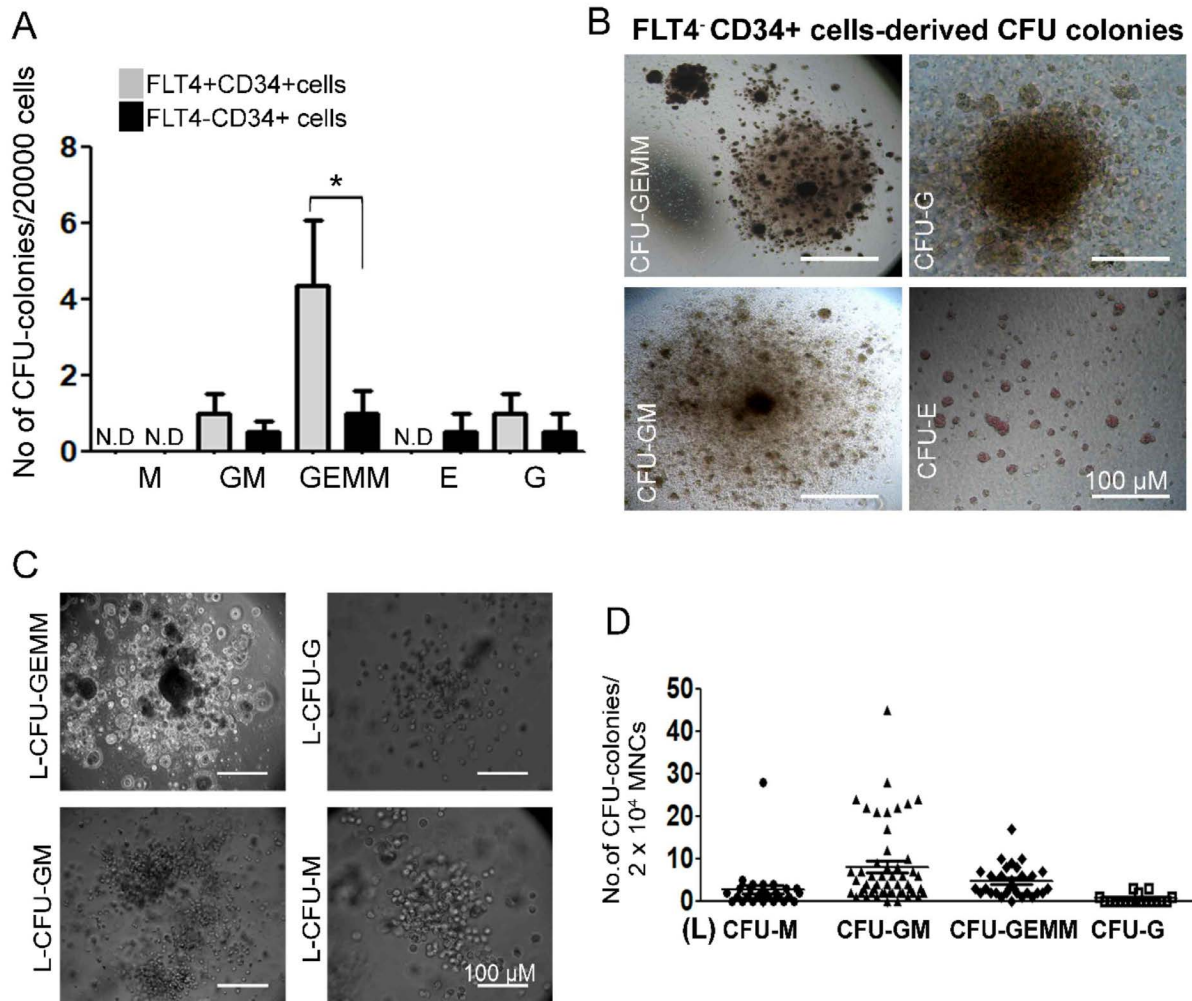
### **Immunostaining**

Immunocytochemistry (ICC) and immunohistochemistry (IHC) were conducted as previously described.<sup>(4)</sup> Cells were initially fixed with 100% methanol for 10 min at room temperature. After washing with PBS, cells were blocked with 5% serum and were subjected to staining with primary antibodies, followed by incubation with secondary antibodies. DAPI (4',6-diamidino-2-phenylindole) was used for nuclear staining and the cells were visualized under a fluorescent microscope (Carl Zeiss, Axiovert 200, Germany) or Zeiss LSM 700 confocal laser scanning microscope and LSM 700 Image software (CLSM, Carl Zeiss, Jena, Germany). For staining of surface and cytosolic FLT4, biotinylated anti-human FLT4 (R&D Systems, BAM3492) and rabbit anti-human FLT4 (ab27278) were used as primary antibodies; FITC-streptavidin conjugated and PE conjugated anti rabbit IgG were used as secondary antibodies in confocal imaging. For western blotting, phospho FLT4 (Cell applications, cy1115), FLT4 (Santa crus, sc-28297), phospho PI3K (Thermo Fisher Scientific, PA5-17387), PI3K (Cell signaling, 4249S), phospho AKT (Cell signaling, 4075S), AKT (Cell signaling, 4691S), GAPDH (Novus Biologicals, NB300-324) and proper secondary goat anti-rabbit IgG-HRP were used in western blotting. For immunohistochemistry, BM samples were fixed in paraformaldehyde (PFA), decalcified with 5% formic acid, and embedded in paraffin. After antigen retrieval, sections were blocked for endogenous peroxidase activity and were incubated with a rat antibody to mouse FLT4 (552857 BD Biosciences). Rabbit anti-rat HRP (P0540, Dako) was used as a secondary antibody. All

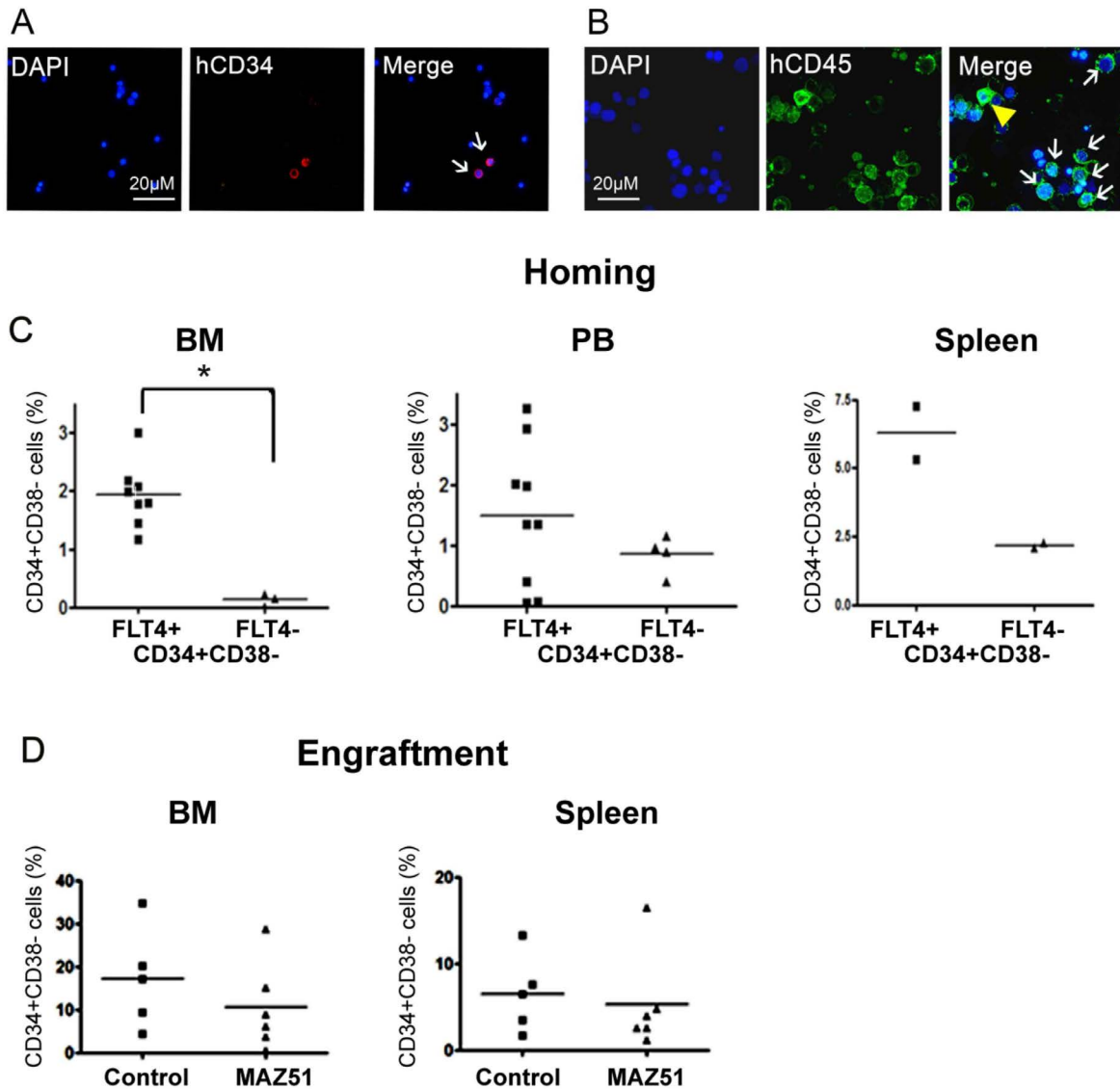
procedures were performed on a DAKO autostainer (DakoAutostainer Plus, Dako, Glostrup, Denmark) at room temperature. Antibodies were detected using DAKO EnVision (K4003, Dako, Glostrup, Denmark) for 30 minutes followed by 10 minutes of the Dako REAL™ DAB + Chromogen (Code K5007, Dako) detection system. Slides were counterstained with Meyer's hematoxylin. To confirm leukemic blast infiltration, hematoxylin and eosin (H&E) staining was used after fixation.

### **Colony-forming unit (CFU) assay**

CFU-assay was performed as previously described.<sup>(5)</sup> To evaluate whether FLT4<sup>+</sup> cells included leukemia progenitors,  $2 \times 10^4$  MNCs or FLT4<sup>+</sup>CD34<sup>+</sup> were suspended in 1 ml of MethoCultGF (H4434, Stem Cell Technologies) and were then cultured for 14 days. The formation of leukemic colonies was monitored and counted under microscopy.



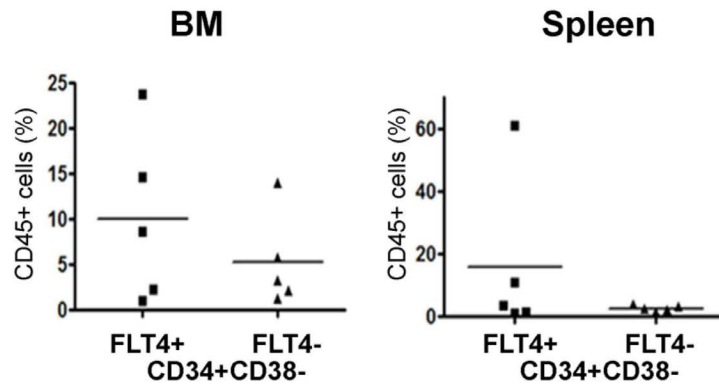
**Supplementary Fig.1. Colony forming unit assays with FLT4<sup>+</sup>CD34<sup>+</sup> cells and FLT4<sup>-</sup>CD34<sup>+</sup> cells.** **A** The number of CFU colonies. n = 4. Each with technical duplicates. \*P < 0.05. Mann–Whitney U test with two-sided P values. **B** Morphologies of different FLT4<sup>+</sup>CD34<sup>+</sup> cells-derived CFU colonies. FLT4<sup>+</sup>CD34<sup>+</sup> cells generated normal morphology colonies such as granulocyte, erythrocyte, monocyte, and megakaryocyte-CFU (CFU-GEMM); granulocyte and macrophage-CFU (CFU-GM); granulocyte-CFU (CFU-G); and macrophage-CFU (CFU-M). Scale bar = 100 μM. **C**. Colony-forming unit (CFU) assays in terms of MAZ51 treatment of leukemic cells. These cells were cultured in methycellulose medium and colonies were counted at 14 days. L-CFU-GEMM: granulocyte, erythrocyte, monocyte, and megakaryocyte-L-CFU. L-CFU-G: granulocyte-L-CFU. L-CFU-GM: granulocyte and macrophage-L-CFU. L-CFU-M: macrophage-L-CFU. Scale bar = 100 μm. **D** Average colony numbers for figure D. n = 10. Each with technical triplicates. \*P < 0.05, \*\*P < 0.01. Mann–Whitney U test with two-sided P values.



**Supplementary Fig.2. Flow cytometric analysis of homed and engrafted CD34<sup>+</sup>CD38<sup>-</sup> cells in BM, PB, and spleen.** **A.** Representative images of BM immunostained for human CD34 (red, white arrows) cells were detected in BM cells. Images from at least 2 independent experiments for each animal are shown. Mann–Whitney U test with two-sided P values. Scale bar = 20 µm. **B.** Images from at least 2 independent experiments for each animal are shown. CD45<sup>dim</sup> (green, white arrows), CD45<sup>high</sup> (green, yellow arrowhead) and DAPI (blue) are demarcated in PB cells. Scale bar = 20 µm. **C** The percentage of homed CD34<sup>+</sup>CD38<sup>-</sup> cells in BM, PB, and spleen of NSG mice injected with FLT4<sup>+</sup>CD34<sup>+</sup>CD38<sup>-</sup> cells or FLT4<sup>-</sup>CD34<sup>+</sup>CD38<sup>-</sup> cells. n = 2-9. Each with technical triplicates. \*P < 0.05. Mann–Whitney U test with two-sided P

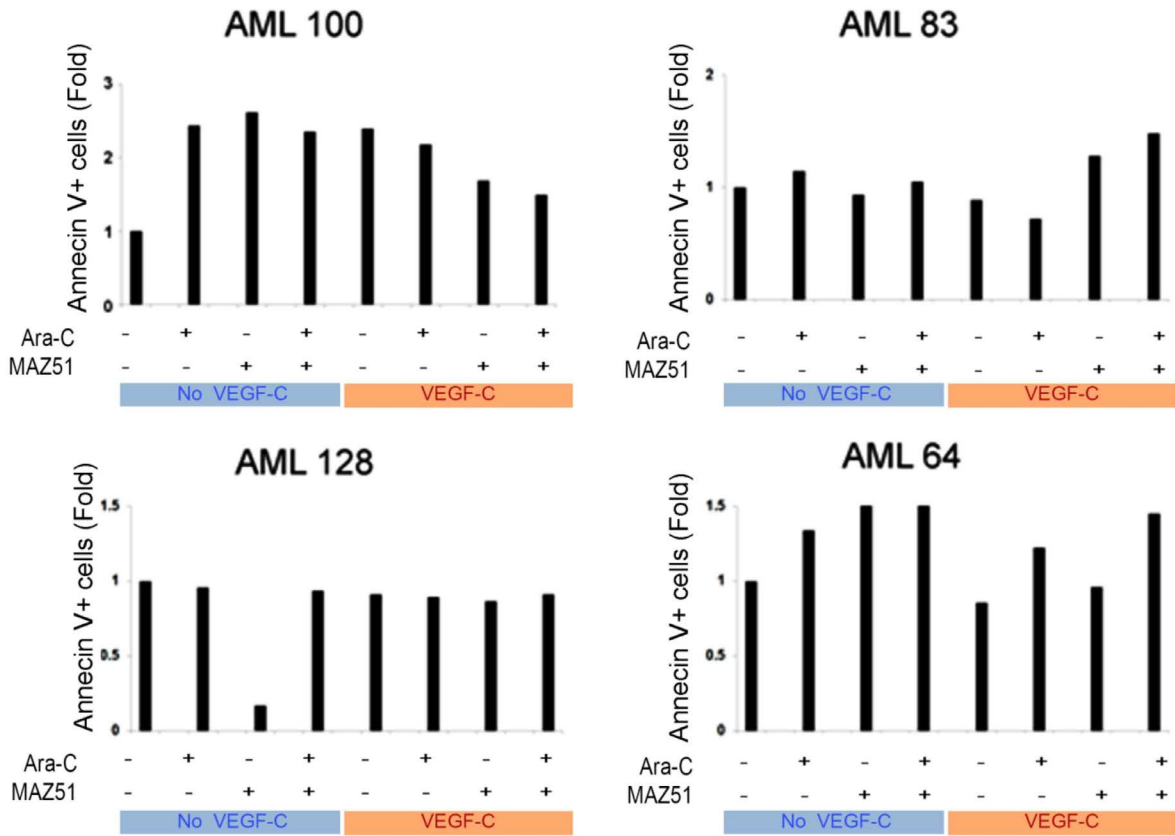
values. **D** Engraftment of CD34<sup>+</sup>CD38<sup>-</sup> cells in BM and spleen measured by flow cytometry; cells were injected into NSG mice after treatment with or without MAZ51. n = 2-3. Each with technical triplicates. Mann–Whitney U test with two-sided P values.

## Engraftment

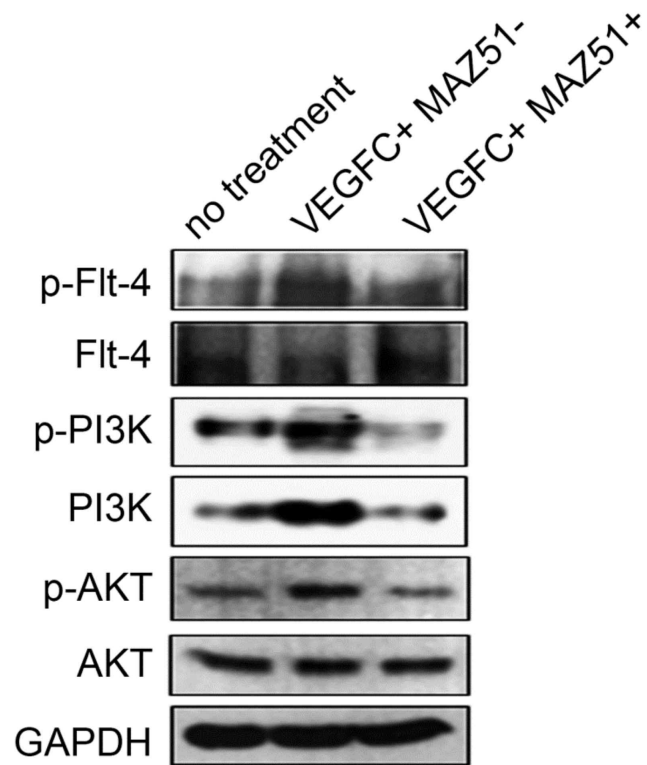


**Supplementary Fig.3. Flow cytometric analysis of engrafted CD34<sup>+</sup>CD38<sup>-</sup> cells in NSG mice.** The percentage of engrafted CD45<sup>+</sup> cells in BM and spleen of NSG mice injected with FLT4<sup>+</sup>CD34<sup>+</sup>CD38<sup>-</sup> cells or FLT4<sup>-</sup>CD34<sup>+</sup>CD38<sup>-</sup> cells. n = 2. Each with technical triplicates. Mann–Whitney U test with two-sided P values.

In CD45<sup>dim</sup>CD34<sup>+</sup>CD38<sup>-</sup> cells from non-refractory patients



**Supplementary Fig.4. No effects of MAZ51 treatment on apoptosis of CD45<sup>dim</sup>CD34<sup>+</sup>CD38<sup>-</sup> cells in non-refractory patients regardless of the presence of VEGF-C.** The fold value of apoptotic cells is shown. The number in the title represents the patient identification number.



**Supplementary Fig.5. Western blot analysis for FLT4, PI3K and AKT including their phosphorylation in Jurkat cells.** MAZ51 inhibits phosphorylation of PI3K and AKT in Jurkat cells. Shown western blot presents that FLT4 expressing Jurkat cells by VEGF-C stimulates PI3K-AKT pathway, results in blasts survival.

**Table S1. Clinical and laboratory features of AML patients**

Patients	Age	Sex	Cell source	WBC/ mm <sup>3</sup> at diagnosis	Cytogenetic anomalies	Status	WHO type
1	19	M	PB	209000	46,XY[20]	de novo AML	M2
2	39	F	PB	3390	46,XX,t(9;11)(p22;q23)[29]/46,XX[1]	de novo AML	MLLT3-KMT2A
3	49	M	PB	1500	43,XY,der(2)t(2;13)(p21;q14),der(3)t(3;13)(q13.2;q13),der(5)t(5;17)(p14;p21)t(5;13)(q13;q14),der(7;17)(q10;p10),t(10;22)(q24;q13),-13,ins(13;5)(q14;q13q31),-18[28]/46,XY[2]	de novo AML	MRC
4	59	F	PB	1130	46,XX[20]	de novo AML	M0
5	54	F	PB	226470	46,XX[10]	de novo AML	NPM1
6	37	M	PB	245000	46,XY[20]	de novo AML	NPM1
7	40	M	PB	510	46,XY,inv(9)(p12q13),i(17)(q10)[6]/46,XY,inv(9)[14]	de novo AML	MRC
8	36	M	PB	108240	46,XY,i(7)(q10)[3]/46,XY[17]	de novo AML	M1
9	65	M	PB	260300	46,XY,del(5)(q11.2q15)[4]/46,XY[16]	de novo AML	MRC
10	36	M	PB	22230	46,XY[20]	de novo AML	MRC
11	81	F	PB	81460	46,XX[20]	de novo AML	M1
12	59	M	PB	2210	46,XY[20]	de novo AML	MRC
13	40	M	PB	12690	46,XY,t(15;17)(q22;q12)[20]	de novo AML	PML-RARA
14	40	M	PB	145710	46,XY,t(15;17)(q22;q21)[20]	de novo AML	PML-RARA
15	66	M	PB	1450	47,XY,der(15)t(15;17)(q22;q12),+17,ider(17)(q10)t(15;17)x2[17]/46,XY[3]	de novo AML	PML-RARA
16	42	M	PB	19490	88~90,XXYY,+X,+X,add(2)(q37),add(3)(q21),del(4)(q31.1),+6,del(6)(q21)x2,-7,-9,-10,-11,-11,-12,-14,+15,add(16)(p13.3),add(16)(q24),-17,add(17)(q25)[cp27]/46,XY[3]	de novo AML	MRC
17	62	F	PB	6860	46,XX[20]	de novo AML	M4
18	46	M	PB	31770	46,XY,t(15;17)(q22;q21)[20]	de novo AML	PML-RARA
19	61	F	PB	62990	46,XY,t(15;17)(q22;q12)[20]	de novo AML	PML-RARA
20	51	F	PB/BM	32130	46,XX[20]	de novo AML	NPM1
21	46	M	PB/BM	46410	46,XY,t(15;17)(q22;q12)[20]	de novo AML	RARA
22	44	F	PB/BM	53940	46,XX[20]	de novo AML	NPM1
23	45	M	PB/BM	4640	46,XY	de novo AML	NPM1
24	52	F	PB/BM	100250	46,XY[20]	de novo AML	NPM1
25	52	F	PB/BM	13430	46,XX[20]	de novo AML	M4
26	53	F	PB/BM	8480	46,XX,inv(9)(p11q13)[20]	de novo AML	M2
27	83	M	PB/BM	2010	46,XY[20]	de novo AML	M2
28	18	F	PB/BM	15880	45,X,-X,t(8;21)(q22;q22)[18]/46,XX[2]	de novo AML	RUNX1-RUNX1T1
29	78	F	PB/BM	196720	46,XX[20]	de novo AML	M5
30	51	M	PB/BM	39630	46,XY,inv(16)(p13.1q22)[20]	de novo AML	CBFB-MYH11
31	79	M	PB/BM	140340	46,X,-Y,+20[16]/45,X,-Y[3]/46,XY[1]	de novo AML	MRC
32	29	M	PB/BM	55030	46,XY,inv(16)(p13.1q22)[4]/48,sl,+4,+8[2]/49,sdl1,+15[11]/50,sdl2,-15,+21,+22[3]	de novo AML	CBFB-MYH11
33	65	M	PB/BM	11650	46,XY[20]	de novo AML	NPM1

34	52	M	PB/BM	3490	46,XY,t(1;20)(p36.1;q13.1),t(2;3)(p23;q27),-7,+mar.ish der(7)(wcp7+)[27]/46,XY[3]	de novo AML	MRC
35	64	M	LPB	17910	47,XY,+4[12]/46,XY[8]	de novo AML	M1
36	65	F	LPB	246900	46,XX[20]	de novo AML	M1
37	79	F	LPB	850	52,XX,+X,+4,del(5)(q31),+8,+9,+10,-15,+17[cp6],46,XX[6]	de novo AML	t-AML(MRC)
38	64	F	LPB	1670	46,XX,der(15)t(15;17)(q22;q12),ider(17)(q10)t(15;17)[16]/46,XX[4]	de novo AML	PML-RARA
39	22	M	LPB	68700	45,X,-X,t(8;21)(q22;q22)[18]/46,XX[2]	de novo AML	RUNX1-RUNX1T1
40	33	F	LPB	10600	45,X,-X,t(8;21)(q22;q22)[18]/46,XX[2]	de novo AML	RUNX1-RUNX1T1
41	51	F	LPB	7790	46,XX[20]	de novo AML	M4
42	44	M	LPB	69740	46,XY,t(15;17)(q22;q12)[19]/46,XY[1]	de novo AML	PML-RARA
43	37	M	LPB	142820	46,XY[20]	de novo AML	M1
44	51	M	LPB	4580	46,XY,del(3)(p?23),del(5)(q13q33),del(5)(q31q35),t(7;19)(q22;q13.3),t(14;17)(q24;p11.2),-18,add(20)(q11.2),+mar,1min[cp14]/47,idem,+mar[5]/46,XY[1]	secondary AML	MRC
45	36	M	LPB	144500	45,XY,der(13;14)(q10;q10)[20]	de novo AML	NPM1
46	41	M	LPB	43010	46,XY,t(15;17)(q22;q12)[20]	de novo AML	PML-RARA
47	68	M	LPB/BM	2030	46,XY[20]	de novo AML	NPM1
48	43	M	LPB/BM	1850	46,XY,inv(16)(p13.3q22)[25]/47,idem,+22[5]	de novo AML	CBFB-MYH11
49	46	M	LPB	14700	46,XY,t(10;11)(p13;q23)[10]/46,XY[20]	de novo AML	KMT2A rearranged
50	64	F	LPB	114510	46,XX[20]	de novo AML	M5
51	36	F	PB/BM	240640	46,XX[20]	de novo AML	NPM1
52	52	M	PB/BM	26670	46,XY[20]	de novo AML	M5
53	48	F	PB/BM	850	43~45,XX,?(1;6)(q21;q21),-3,add(3)(q25),-5,-7,del(10)(q24),add(17)(p11.2),add(18)(q23),+mar1,+mar2[cp16]/46,XX[4]	treatment related	MRC
54	30	M	PB/BM	44730	46,XY,t(8;21)(q22;q22)[19]/46,XY[1]	de novo AML	RUNX1-RUNX1T1
55	27	M	PB/BM	2150	46,XY,t(9;11)(p22;q23)[26]/46,idem,add(1)(p36.1)[4]	de novo AML	MLLT3-KMT2A
56	45	M	PB/BM	71820	46,XY,inv(16)(p13.1q22)[20]	de novo AML	CBFB-MYH11
57	23	F	PB/BM	24420	46,XX,inv(9)(p11q13)[20]	de novo AML	M1
58	27	F	PB/BM	20620	46,XX,t(8;21)(q22;q22)[23]/45,idem,-X[6]/46,XX[1]	de novo AML	RUNX1-RUNX1T1
59	41	F	PB/BM	142700	46,XX,t(6;11)(q27;q23)[30]	de novo AML	KMT2A rearranged
60	28	F	PB/BM	12800	46,XX,t(6;11)(q27;q23)[19]/46,XX[1]	de novo AML	KMT2A rearranged
61	58	M	PB/BM	317620	46,XY[20]	de novo AML	M4
62	65	F	PB/BM	141720	46,XX[20]	de novo AML	NPM1
63	72	M	PB/BM	114700	46,XY[5]	de novo AML	M4
64	56	M	LPB	34740	46,XY[20]	de novo AML	NPM1
65	33	F	LPB	2690	45,X,-X,t(8;21)(q22;q22)[16]/46,idem,+X[3]/46,XX[1]	de novo AML	RUNX1-RUNX1T1
66	39	M	LPB	141200	47,XY,+mar[3]/46,XY[22]	de novo AML	M4
67	41	F	LPB	143720	46,XX,t(6;11)(q27;q23)[20]	de novo AML	KMT2A

68	53	M	LPB	42060	46,XY,t(15;17)(q22;q12)[20]	de novo AML	rearranged PML-RARA
69	84	F	LPB	51840	46,XX[20]	de novo AML	M5
70	48	M	LPB	148800	47,XY,+11[29]/46,XY[1]	de novo AML	M1
71	27	M	LPB	147800	46,XY[20]	de novo AML	M5
72	31	M	LPB	154500	46,XY,t(9;22)(q34;q11.2),inv(16)(p13.1q22)[13]/47,idem,+17[15]/48,idem,+8,+17[2]	de novo AML	CBFB
73	18	M	LPB	101220	46,XY,der(9)del(p13p22)inv(p12q13)[18]/46,XY[2]	de novo AML	MRC
74	25	M	LPB	172240	46,XY[20]	de novo AML	M1
75	63	F	LPB	10070	46,XX[20]	de novo AML	NPM1
76	16	F	LPB	9800	46,XX,t(2;21;8)(q37;q22;q22)[27]/46,XX[3]	de novo AML	RUNX1- RUNX1T1
77	46	M	LPB	108400	46,XY,inv(16)(p13.1q22)[20]	de novo AML	CBFB
78	19	M	LPB	113010	46,XY[20]	de novo AML	NPM1
79	50	F	LPB	1340	46,XX,inv(9)(p11q13)[20]	de novo AML	M1
80	41	F	LPB	8280	46,XX[20]	de novo AML	MRC
81	77	F	LPB	124680	46,XX,del(9)(q13q22)[20]	de novo AML	M4
82	67	M	LPB	7750	46,XY	de novo AML	MRC
83	31	M	LPB	6850	46,XY,t(15;17)(q22;q12)[20]	de novo AML	RARA
84	65	F	LPB	246900	46,XX[20]	de novo AML	M1
85	31	M	LPB/B M	154500	46,XY,t(9;22)(q34;q11.2),inv(16)(p13.1q22)[13]/47,idem,+17[15]/48,idem,+8,+17[2]	de novo AML	CBFB
86	64	M	BM	251370	46,XY[20]	de novo AML	M1
87	60	F	BM	12700	46,XX,+2~42dmin[10]/47,idem,+4[14]/47,XX,+mar[4]/46,XX[2]	de novo AML	MRC
88	40	F	BM	38200	46,XX,add(7)(q22)[cp2]/46,XX[18]	de novo AML	MRC
89	59	M	BM	62260	46,XY,der(17)t(11;17)(q13q23;q25)[19]/46,XY[1]	de novo AML	KMT2A rearranged
90	47	F	BM	6980	47,XX,del(9)(q21q22),t(16;21)(p11.2;q22),+22[4]/48,idem,+X[2]/48,idem,+10[4]/49,idem,+10,+18[4]/49,idem,+10,+20[4]/51,idem,+X,+5,+10,+11[2]	de novo AML	NPM1
91	59	F	BM	27450	47,XX,+8[7]/46,XX[13]	de novo AML	M1
92	55	F	BM	1770	46,XX[20]	de novo AML	M1
93	58	F	BM	360620	46,XX,t(3;3)(q21;q26.2),del(7)(q22q32),add(16)(q22)[20]	de novo AML	GATA2- MECOM
94	64	M	BM	7840	47,XY,+8[19]/46,XY[1]	de novo AML	M1
95	72	F	BM	13570	46,XX,t(9;11)(p21;q23)[19]/46,XX[1]	de novo AML	MLLT3- KMT2A
96	33	F	BM	122390	46,XX[20]	de novo AML	M5
97	43	F	BM	33120	46,XX[20]	de novo AML	M5
98	65	F	BM	31700	46,XX,t(9;11)(p21;q23)[20]	de novo AML	MLLT3- KMT2A
99	83	F	BM	45330	47,XX,+8[9]/47,idem,+8,-10,add(17)(p11.2)[7]/46,XX[4]	de novo AML	MRC
100	46	M	BM	86080	47,XY,+X[20]	de novo AML	M1
101	42	M	BM	81410	46,XY,t(3;12)(q27;p13)[19]/46,XY[1]	de novo AML	NPM1
102	19	M	BM	7340	45,X,-Y,t(8;21)(q22;q22)[20]	de novo AML	RUNX1- RUNX1T1
103	35	F	BM	18060	46,XX,inv(9)(p11q12)[20]	de novo AML	M1
104	60	M	PB	1750	46,XY,t(9;11)(p22;q23)[4]/46,XY[16]	CR	MLLT3- KMT2A

105	57	M	PB	374180	46,XY,inv(16)(p13.1q22)[20]	CR	CBFB
106	48	M	PB	116330	46,XY[20]	CR	M1
107	61	F	PB	170180	46,XX[20]	CR	M5
108	49	M	PB	22220	46,XY[20]	CR	M5
109	52	M	PB	1840	46,XY[20]	CR	M1
110	57	F	PB	194120	46,XX[20]	CR	M1
111	47	F	PB	3170	46,XX[20]	CR	MRC
112	61	F	LPB/B M	30090	46,XX,t(9;11)(p22;q23)[20]	CR	MLLT3- KMT2A
113	26	M	PB	14700	46,XY,t(6;11)(q27;q23)[1]/46,XY[2 9]	CR	KMT2A rearranged
114	47	F	PB	3170	46,XX[20]	CR	M1
115	59	M	BM	82280	inv(16)(p13.1q22);CBFB-MYH11	CR	CBFB
116	63	M	BM	2150	47,XX,inv(16)(p13.1q22),+22[30]	CR	M5
117	24	M	BM	31650	45,X,-Y[20]	CR	MLLT3- KMT2A
118	68	F	BM	50400	46,XY,t(9;11)(p22;q23)[20]	CR	MRC
119	38	M	BM	14410	46,XX[20]	CR	RUNX1- RUNX1T1
120	56	M	BM	24110	Y,t(8;21)(q22;q22)[23]/47,XYc,t(8 ;21)(q22;q22)[7]	CR	M5
121	43	F	BM	9310	46,XY[20]	CR	M4
122	52	F	PB	129860	46,XX,t(16;21)(q24;q22)[20]	SCT	MRC
123	69	M	PB	88020	46,XX[20]	SCT	NPM1
124	51	F	PB	31430	46,XY[20]	SCT	M2
125	31	F	PB	100180	46,XX,del(9)(q13q22)[21]/46,XX[9]	SCT	M2
126	56	F	PB	2350	46,XX,t(11;19)(q23;p13.1)[25]/46,i dem,del(12)(p13)[3]/46,XX[2]	SCT	KMT2A rearranged
127	59	M	PB	82280	inv(16)(p13.1q22);CBFB-MYH11	SCT	CBFB
128	65	M	PB	640	47,XX,inv(16)(p13.1q22),+22[30]	SCT	M1
129	31	F	PB	1380	46,XY[20]	SCT	M5
130	34	M	PB	147800	46,XX[20]	SCT	M5
131	65	F	PB/BM	6710	46,XY[20]	Refractory	MRC
132	63	F	PB/BM	3470	46,XX[10]	Refractory	M7
133	55	F	PB/BM	26000	46,XX[20]	Refractory	M2
134	78	M	PB/BM	2200	46,XY[20]	Refractory	M2
135	54	M	PB/BM	3160	47,XY,+8[19]/46,XY[1]	Refractory	M4
136	63	F	PB/BM	3470	46,XX[10]	Refractory	NPM1
137	58	M	PB/BM	198890	46,XY,del(9)(q13q21)[13]/46,XY[7]	Refractory	NPM1
138	61	F	LPB/B M	30090	46,XX,t(9;11)(p22;q23)[20]	Refractory	MLLT3- KMT2A
139	72	M	LPB/B M	60450	46,XY[20]	Refractory	M4
140	37	M	PB	142820	46,XY[20]	Refractory	M2
141	45	F	PB/BM	23450	46,XY[21]	Refractory	M1
142	32	F	PB/BM	678234	46,XY[22]	Refractory	M1
143	48	M	LPB/B M	11860	46,XY[20]	Relapsed	NPM1
144	47	F	LPB/B M	143720	46,XX,t(6;11)(q27;q23)[20]	Relapsed	KMT2A rearranged
145	46	M	PB	108400	46,XY,inv(16)(p13.1q22)[20]	Relapsed	CBFB
146	77	F	PB	124680	46,XX,del(9)(q13q22)[20]	Relapsed	M4
147	50	F	PB	1340	46,XX,inv(9)(p11q13)[20]	Relapsed	M1

Abbreviation : AML, acute myeloid leukemia; WBC, white blood cell; PB, peripheral blood; BM, bone marrow

**Table S2. Primers and probes for quantitative RT-PCR**

Genes		Primers and probes (5'-3')
human <i>GAPDH</i>	Forward	GGTGGTCTCCTCTGACTTCAACA
	Reverse	GTGGTCGTTGAGGGCAATG
	Probe	CCACTCCTCCACCTTTGACGCTGG
human <i>FLT4</i>	Forward	CCTTGCCCGGGACATCTA
	Reverse	TTGTCTGAAGATGCTTTCAGGG
	Probe	AGACCCCGACTACGTCCGCAAGG
human <i>LYVE-1</i>	Forward	CTGGGTTGGAGATGGATTCTG
	Reverse	TCAGGACACCCACCCCATTT
	Probe	TAGCCCAAACCCCAAGTG
human <i>PDPN</i>	Forward	CAGGTGCCGAAGATGATGTG
	Reverse	TGTTGCCACCAGAGTTGTCA
	Probe	TGACTCCAGGAACCAG
human <i>PROX-1</i>	Forward	GCCAGATTTGCAGTCAATGG
	Reverse	ATGATGACGTCGCCAAAGC
	Probe	TTTCCACACCGCCAAC
human <i>CXCR4</i>	Forward	TGGGTGGTTGTGTTCCAGTTT
	Reverse	ATGCAATAGCAGGACAGGATGA
	Probe	CATGGTTGGCCTATCCTGCCTGGTA
human <i>CD56</i>	Forward	CAAGTGTGGCCTGTTCATGTG
	Reverse	GGGCCCCGGCTTTTCC
	Probe	ATTGCGGTCAACCTGT
human <i>VEGF-C</i>	Forward	GTGTCAGGCAGCGAAGAC
	Reverse	CTGAGCCAGGCATCTGCAG
	Probe	TGCCCCACCAATTACATGTGGAATAATCA

## Reference

1. Lee JY, Park S, Min WS, et al. Restoration of natural killer cell cytotoxicity by VEGFR-3 inhibition in myelogenous leukemia. *Cancer Lett.* 2014 ;354(2):281-9.
2. Han AR, Lee JE, Lee MJ, et al. Distinct Repopulation Activity in Hu-Mice Between CB- and LPB-CD34(+) Cells by Enrichment of Transcription Factors. *Int J Stem Cells.* 2021 ;14(2):203-11.
3. Jeon SB, Han AR, Choi YB, et al. Lymphoid Lineage gammadelta T Cells Were Successfully Generated from Human Pluripotent Stem Cells via Hemogenic Endothelium. . *Int J Stem Cells.* 2023 ;16(1):108-16.
4. Lee JY, Park S, Kim DC, et al. A VEGFR-3 antagonist increases IFN-gamma expression on low functioning NK cells in acute myeloid leukemia. *J Clin Immunol.* 2013 ;33(4):826-37.
5. Jeon SB, Han AR, Lee S, et al. CD34(dim) cells identified as pluripotent stem cell-derived definitive hemogenic endothelium purified using bone morphogenetic protein 4. *Cell Prolif.* 2023 ;56(2):e13366.

**Supplementary Information** – Pagano, Fernandez-Botana, *et al.*

**Interleukin-27 potentiates CD8<sup>+</sup> T cell-mediated anti-tumor immunity in Chronic Lymphocytic Leukemia**

**Materials and Methods**

**Animal experiments**

Leukemic cells derived from *Eμ-TCL1* mice were adoptively transferred (AT) by i.p. or i.v. transplantation ( $1-2 \times 10^7/100\mu\text{l}$  DMEM) into C57BL/6 wild type (WT), *Ebi3*<sup>-/-</sup> (Jax #008691), and *Rag2*<sup>-/-</sup> mice. All murine lines used were of C57BL/6 background. In specific experiments, CLL cells were injected after isolation from the spleen using the MojoSort™ Mouse Pan B Cell Isolation Kit (Biolegend) according to the manufacturer's instructions. Unless stated otherwise, all AT experiments were performed on sex and age-matched mice ranging from six to ten weeks of age. When applicable, CD3<sup>+</sup> T-cells were isolated from WT and *Ebi3*<sup>-/-</sup> splenocytes using the MojoSort™ Mouse CD3 T-cell Isolation Kit (Biolegend) according to the manufacturer's instructions, and co-injected with the *Eμ-TCL1* splenocytes. CLL progression in leukemic mice was monitored weekly by assessment of the percentage of CD5<sup>+</sup> CD19<sup>+</sup> cells in the PB. The blood cell count was determined using the MS4e Vet haematology analyser (Melet-Schloesing, France).

Mice were euthanized by cervical dislocation before reaching the established humane end-point, and the leukemic spleens were dissected and processed as previously described.

*In vivo* treatment with IL-27 neutralizing antibody or isotype IgG control (BioXcell, NH) was performed *i.p.* in *Eμ-TCL1*-AT mice. Antibody administration started two days prior to CLL AT and was repeated twice a week throughout the course of the experiment. For the first two injections, 500μg of anti-IL-27 neutralizing antibody were administered per mouse in 200μl of buffer (Day -2 and day 0). The following injections comprised 250μg of anti-IL-27 antibody in 100μl buffer. Blood serum was obtained weekly during routine blood checks by centrifuging the coagulated PB (2000g, 4°C, 20').

## **Flow cytometry**

### Cell sorting

CD3<sup>+</sup> T-cells were isolated from *FoxP3<sup>YFP/Cre</sup>* (Jax #016959, C57BL/6 background) and *FoxP3<sup>YFP/Cre</sup> Ebi3<sup>-/-</sup>* mice using MojoSort™ Mouse CD3 T-cell Isolation Kit (Biolegend), and activated with plate-bound anti-CD3 (2µg/ml), anti-CD28 (2µg/ml) and IL-2 (10 ng/mL) for 72 hours. Cells were harvested after three days, stained for surface markers and FACS-sorted using a FACSAria sorter III (BD Biosciences) in three fractions: CD8<sup>+</sup> T-cells, CD4<sup>+</sup> conventional T-cells and FOXP3<sup>+</sup> regulatory T-cells (Treg, YFP<sup>+</sup>). The samples were immediately spun down (500g, 10'), resuspended in 500 µl of Nucleozol (Takara Bio) and frozen at -80°C.

### Cell clustering

Clustering analysis of live lymphocytes was performed with Cytosplore software. Briefly, samples were randomly down-sampled and subjected to Hierarchical Stochastic Neighbor Embedding (HSNE) to generate clusters based on phenotypic similarities. Clusters were generated using the Gaussian mean shift algorithm using the density estimate as input.

## **T-cell-mediated cytotoxicity assay on murine CLL**

Assessment of the cytotoxicity of IL-27-treated T-cells on murine CLL cells was performed as previously described [1]. Briefly, CD3<sup>+</sup> T-cells were isolated from C57BL/6 mice, cultured in RPMI1640 medium supplemented with 10% FBS, 1% P/S, and stimulated with coated anti-CD3 (1µg/ml) and soluble anti-CD28 (1µg/ml) for 48h at 37°C. Treatment with IL-27 was performed daily (25ng/ml). CLL cells (CD5<sup>+</sup>CD19<sup>+</sup>) isolated from *Eµ-TCL1* mice were stained with CellTrace CFSE (200nM, Thermo Fisher) and pulsed with 2µg/ml of super antigen (sAg; SEA and SEB; Sigma-Aldrich) for 30' at 37°C. The generated target CLL cells (2.5x10<sup>4</sup>) were then loaded with sAg were added to the pre-treated CD3<sup>+</sup> T cells at a 1:20 (target: effector). Cell mixtures were centrifuged, and incubated for 4h at 37°C. Cells were stained with TO-PRO-3 viability dye (Thermo Fisher) according to the manufacturer's instructions and T-cell-mediated cytotoxicity against CLL target cells was determined by flow cytometry. Cytotoxicity was

calculated as: % target cell death = (% CFSE+ TO-PRO-3+ target cells incubated with effector T-cells - % of CFSE+ TO-PRO-3+ target cells incubated alone) × 100/(100 - % of CFSE+ TO-PRO-3+ target cells incubated alone).

### **T-cell-mediated cytotoxicity assay on patient-derived CLL samples**

CLL patient-derived peripheral blood mononuclear cells (PBMCs) were divided into either “target cells” or cells for further processing. The latter were depleted from CD19<sup>+</sup> cells using a positive selection kit, enriched for CD3<sup>+</sup> T cells, and plated with or without IL-27 (100 ng/mL) antibody in 48-well plates previously coated with 1 µg/mL anti-CD3 antibody for 48 h at 37°C.

Prior to the cytotoxicity assay, the target cell fraction CLL cells were stained with CellTrace CFDA (200 nM) (Thermo Fisher) and pulsed with 1 µg/mL of sAgs (SEA and SEB) for 30 min at 37°C. Target cells (2.5x10<sup>4</sup>) loaded with sAg were then added to the pre-treated effector T cells at a 1:20 (target:effector) ratio. Cell mixtures were centrifuged, and the cell pellets incubated for 4 h at 37°C. Target cells from each patient were centrifuged and incubated alone as a control for spontaneous/drug-induced cell death. Finally, cells were stained with TO-PRO-3 viability dye (Thermo Fisher) according to the manufacturer’s instructions and T cell-mediated cytotoxicity against target cells was determined by flow cytometry. Cytotoxicity was calculated as: % target cell death = (% CFDA+ TO-PRO-3+ target cells incubated with effector T cells - % of CFSE+ TO-PRO-3+ target cells incubated alone) × 100 / (100 - % of CFDA+ TO-PRO-3+ target cells incubated alone).

### **Three-dimensional killing assay on human samples**

The real-time killing assay was performed as previously described [2]. In summary, Human CD3/CD28 activator beads (ThermoFisher Scientific) were used to stimulate PBMCs (0.7:1 ratio Beads/PBMCs) with or without IL-27 (100 ng/ml) for 6 days at 37 °C with 5% CO<sub>2</sub>. On day 4, half of the media was replaced by fresh media. For the 3D killing assay, NALM6-pCasper cells [3] were pulsed with SEA and SEB (1µg/ml) at 37 °C with 5% CO<sub>2</sub> for 30 min. The pulsed NALM6-pCasper cells were then embedded

into 2 mg/mL Type I bovine collagen (Advanced Biomatrix) and centrifuged down to the bottom as described before [2]. After gel solidification, PBMCs were placed on top of the collagen matrix at a 20:1 effector: target ratio. Live cell imaging was carried out using a high-content imaging system (ImageXpress, Molecular Devices) at 37 °C with 5% CO<sub>2</sub> for 30 hours. Images were analyzed with ImageJ.

### **RNA sequencing**

Previously sorted cells were thawed and RNA was isolated using the Nucleosol RNA isolation kit (Macherey-Nagel) prior to bulk-RNAseq. Libraries were prepared with the QuantSeq 3' mRNA-Seq Library Prep Kit FWD for Illumina (Lexogen), according to manufacturer's instructions, with the addition of UMI. Barcoded samples were pooled, diluted, loaded onto a NextSeq 500/500 Mid Output flowcell (130M reads, Illumina) and single-end sequencing was performed on a NextSeq 550 (Illumina).

### RNA sequencing analysis

After initial QCs using FastQC and FastQ Screen tools made available by the Babraham Bioinformatics group (<https://www.bioinformatics.babraham.ac.uk/projects>), fastq files were processed using a local Snakemake workflow including the following main steps. First, raw reads were trimmed from their UMI index, poly A and adapter sequences using a combination of dedicated scripts and cutadapt (v2.10). Next, filtered reads were submitted for mapping (STAR v2.5.3a) on the Mouse Reference genome (GRCm38). Collapsing of reads originating from the same fragment was achieved with umi\_tools (v1.0.0) and counting was performed with featureCounts (subread v2.0.0).

Counts were filtered and transformed with EdgeR for clustering and principal component analysis (PCA). Differential expression of genes (DEG) across CD8<sup>+</sup> T-cells, Tconv and Treg cell samples was assessed using the NOISeq R/Bioconductor packages, and a FDR of 0.05 and a log<sub>2</sub> fold change cut-off of 1 were imposed.

## **Immunofluorescence**

$1 \times 10^6$  cells were transferred in a U-bottom 96 well plate. PFA was added at a final concentration of 3.7%. After 15min of incubation at RT, the cells were washed with PBS, and centrifuged at 500g for 5min. Cells were permeabilized with 0.5% Triton x-100 in PBS for 15min at RT. After 2 washes with PBS, cells were blocked with the blocking buffer (1% BSA, 0.5% Triton X-100 in PBS) for 1h at RT. After washes, cells were incubated o.n. with the primary antibodies diluted in blocking buffer (anti-Profilin1, Cell Signalling, #3237, AB\_2236990 and anti-CD8, Biolegend, #100705, AB\_312744).

After 3 washes of 10min in permeabilization buffer, the cells were incubated 1h at RT with the secondary antibodies. The cells were then washed 3 times for 10min in permeabilization buffer. DAPI and actistain were added in the second wash. The cells were resuspended in Ibdid mounting medium and let to settle for 24h at 4°C in an Ibdid chamber ( $\mu$ -Slide angiogenesis). Images were acquired on a confocal laser scanning microscope (LSM810; Zeiss) and analyzed with ImageJ.

## **Cytokine measurements**

The levels of IL-27 in patient blood serum, as well as in murine blood serum and spleen plasma were quantified by ELISA using the LEGEND MAX™ Human IL-27 ELISA Kit (Biolegend) and LEGEND MAX™ Mouse IL-27 Heterodimer ELISA Kit (Biolegend), respectively, according to the manufacturer's instructions. Equal volumes of serum or spleen plasma were loaded across conditions.

## **Real-time PCR**

### Cell populations sorting

Leukemic C57BL/6 wild type (WT), previously AT with *E $\mu$ -TCL1*-derived splenocytes, were euthanized before reaching the humane end-point and the leukemic spleens were dissected and processed. Cell suspensions were then stained for surface markers and sorted into five fractions using a Symphony sorter (BD Biosciences): CLL cells (CD19<sup>+</sup>), CD8<sup>+</sup> T-cells (CD19<sup>-</sup> NK1.1<sup>-</sup> CD3<sup>+</sup>CD8<sup>+</sup>CD4<sup>-</sup>) CD4<sup>+</sup> T-cells (CD19<sup>-</sup>

NK1.1<sup>-</sup>CD3<sup>+</sup>CD8<sup>-</sup>CD4<sup>+</sup>), dendritic cells (CD19<sup>-</sup>NK1.1<sup>-</sup>Ly-6G<sup>-</sup>CD11c<sup>+</sup>CD11b<sup>+</sup>) and monocytes/macrophages (CD19<sup>-</sup>NK1.1<sup>-</sup>Ly-6G<sup>-</sup>CD11c<sup>-</sup>CD11b<sup>+</sup>). The sorted populations were immediately spun down (500g, 10min), resuspended in Nucleozol and frozen at -80°C.

### RNA isolation

RNA from whole splenocytes or sorted cell types was isolated using the NucleoSpin RNA Set for NucleoZOL Mini kit according to manufacturer's instructions (Macherey-Nagel) and quantified with Nanodrop (Thermo Scientific).

### Gene expression in cells

Reverse transcription of mRNA was performed in a SimpliAmp™ Thermal Cycler (ThermoFisher) using FastGene® Scriptase II cDNA 5x ReadyMix (Nippon genetics). Real-time PCR was performed in the QuantStudio™ 5 Real-Time PCR System (ThermoFisher) using the Takyon Low Rox SYBR 2XMaster Mix blue dTTP (Eurogentec). The primer sequences were as follows: *Ebi3* F: 5'- CTTCTCGGTATCCCGTGGC - 3' and R: 5'- ACCGAGCCTGTAAGTGGCAAT -3', *Il27p28* F: 5'- TGTCACAGCTTTGCTGAAT-3' and R: 5'- CCGAAGTGTGGTAGCGAGG-3', *18S* F: 5'- CCGCCGCATGTCTCTAGT-3' and R: 5'- CTTTCCTCAACACCACATGAGC-3'

### **Analysis of publicly available data sets**

For the analysis of *Ebi3* gene expression, we collected raw or processed data from the GSE18026, GSE35179, GSE66858, GSE8835, and GSE8836 datasets (GEO database, NCBI). We used gene expression data from several CD8<sup>+</sup> T-cell populations for comparison [4]. Expression of differentially expressed genes from clusters 1-10 was gathered for PCA and clustering analysis.

1. Ioannou, N., et al., *Triggering interferon signaling in T cells with avadomide sensitizes CLL to anti-PD-L1/PD-1 immunotherapy*. *Blood*, 2021. **137**(2): p. 216-231.
2. Zhao, R., et al., *Targeting the Microtubule-Network Rescues CTL Killing Efficiency in Dense 3D Matrices*. *Front Immunol*, 2021. **12**: p. 729820.
3. Knorck, A., et al., *Cytotoxic Efficiency of Human CD8(+) T Cell Memory Subtypes*. *Front Immunol*, 2022. **13**: p. 838484.
4. Beltra, J.C., et al., *Developmental Relationships of Four Exhausted CD8(+) T Cell Subsets Reveals Underlying Transcriptional and Epigenetic Landscape Control Mechanisms*. *Immunity*, 2020. **52**(5): p. 825-841 e8.

## Figure legends

**Figure S1: *Ebi3*<sup>-/-</sup> transgenic mice do not produce IL-27 and display a TME with immunosuppressive features.**

**(A)** Relative mRNA levels of the IL-27 subunits, p28 and *Ebi3*, in splenocytes of WT and *Ebi3*<sup>-/-</sup> mice. **(B)** Number of circulating neoplastic CD5<sup>+</sup> CD19<sup>+</sup> cells (n=18 for Ctrl and n=19 for *Ebi3*<sup>-/-</sup>, two-way ANOVA), same mice as Fig 1A. **(C)** Experimental scheme and relative mRNA levels of the IL-27 subunits (*Ebi3* and *Il27p28*) in murine CLL cells, CD8<sup>+</sup> T cells, CD4<sup>+</sup> T cells, dendritic cells, monocytes/macrophages (relative to the housekeeping gene 18S) sorted from the spleen of leukemic mice (AT with TCL1 splenocytes; n=4). **(D-I)** The data shown corresponds to one experimental cohort of AT mice (n=9 for Ctrl and n=10 for *Ebi3*<sup>-/-</sup>) as for Fig.1B-F **(D)** Cell numbers of CD8<sup>+</sup> T cells, CD4<sup>+</sup> Tconv, and Tregs in the spleen are compared between the two groups. **(E)** HSNE plots (Cytosplore) and heatmap depicting the expression of CD44, Ki-67, PD1, IFN- $\gamma$ , TIGIT and CD62L on Ctrl and *Ebi3*<sup>-/-</sup> CD8<sup>+</sup> T cells. **(F)** Percentages of CD8<sup>+</sup> T-cell cluster distribution in Ctrl and *Ebi3*<sup>-/-</sup> CD8<sup>+</sup> T cells. **(G)** Frequency of CD4<sup>+</sup> Tconv with a naive (CD62L<sup>+</sup> CD44<sup>-</sup>), effector (CD62L<sup>-</sup> CD44<sup>+</sup>) or memory (CD62L<sup>+</sup> CD44<sup>+</sup>) phenotype among Ctrl and *Ebi3*<sup>-/-</sup> mice. **(H)** HSNE plots (Cytosplore) and heatmap depicting the expression of CD44, Foxp3, Ki-67, PD-1, IFN- $\gamma$ , TIGIT and CD62L expression measured by FC on Ctrl and *Ebi3*<sup>-/-</sup> CD4<sup>+</sup> T cells. **(I)** Percentages of cluster distribution on Ctrl and *Ebi3*<sup>-/-</sup> CD4<sup>+</sup> T cells. Unpaired t test, \*  $P < .05$ , \*\*  $P < .01$ , \*\*\*  $P < .001$ , \*\*\*\*  $P < .0001$ .

**Figure S2: EBI3 depletion does not affect myeloid cell compartment and mildly affects T-cell distribution in a non-tumoral context.**

**(A-F)** Healthy *Foxp3*<sup>YFP/Cre</sup> and *Foxp3*<sup>YFP/Cre</sup> *Ebi3*<sup>-/-</sup> mice (n=3 per group) were euthanized at 8 weeks of age and their splenocytes analyzed using FC. **(A)** Frequency of indicated cell populations among total live cells. T= T cells; NK= Natural killer cells; NKT= natural killer T cells; Myelo= myeloid cells. **(B)** Frequency of indicated cell populations out of CD11b<sup>+</sup> cells. Neutro=neutrophils; DCs=dendritic cells; Mono=monocytes; Macro=macrophages. **(C)** Frequency of T-cell subpopulations among total T cells.

**(D-F)** CD8<sup>+</sup> and CD4<sup>+</sup> T cells were isolated from *Foxp3<sup>YFP/Cre</sup>* and *Foxp3<sup>YFP/Cre</sup> Ebi3<sup>-/-</sup>* splenocytes, stimulated *ex vivo* with PMA (80nM), ionomycin (1,3 mM) and brefeldin A (5µg/ml) and analyzed by FC. Frequency of indicated immune checkpoints and cytokines in **(D)** CD8<sup>+</sup> effector T cells, **(E)** CD4<sup>+</sup> Tconv cells and **(F)** Tregs after *ex vivo* stimulation. Unpaired t test, \*\* *P* < .01.

**Figure S3: EBI3 depletion in transgenic Eµ-TCL1 mice promotes an immunosuppressive TME.**

**(A)** Number of circulating leukemic cells in T and TE mice (n=17 in T mice and n=14 in TE mice). **(B-J)** Leukemic T and TE mice were euthanized and their splenocytes were processed and analyzed by FC (n=5 in T mice and n=6 in TE mice). **(B)** Percentage of CLL cells among splenocytes of T and TE mice. **(C)** Number of CLL cells in the spleen of T and TE mice. **(D)** Heatmap and HSNE plots depicting the expression of individual markers included in the clustering analysis of CD8<sup>+</sup> T cells derived from T and TE transgenic mice based on the expression of CD44, Ki-67, PD1, KLRG1, TIGIT, and CD62L measured by FC. **(E)** Percentages of CD8<sup>+</sup> T-cell clusters distribution on T and TE. **(F)** Percentage of CD4<sup>+</sup> T cells in the spleen of T and TE transgenic mice. **(G-H)** HSNE clustering analysis of T and TE CD4<sup>+</sup> T cells based on the expression of CD44, FOXP3, Ki-67, PD1, KLRG1 and CD62L measured by FC. Heatmap comprising the clusters and HSNE plots depicting the expression of individual markers. **(I)** Percentages of cluster distribution in CD4<sup>+</sup> T cells in T and TE mice. **(J)** CLL cells were isolated from T and TE mice (n=3 mice per group) and activated for 48h *in vitro*. CLL cells were stained and analyzed by FC. Unpaired t test, \* *P* < .05, \*\* *P* < .01.

**Figure S4: Specific T-cell-EBI3 depletion leads to a more immunosuppressive TME.**

**(A)** Number of circulating T cells in recipient *Rag2<sup>-/-</sup>* mice injected with either Ctrl or *Ebi3<sup>-/-</sup>* CD3<sup>+</sup> T cells. **(B)** HSNE clustering analysis of Ctrl and *Ebi3<sup>-/-</sup>* CD8<sup>+</sup> T cells based on PD1, CD25, LAG3, CD127, TIGIT and CD44 expression measured by FC. Heatmap comprising the clusters generated by HSNE analysis and HSNE plots depicting the expression of individual markers. **(C)** Percentages of cells in clusters from CD8<sup>+</sup> T cells isolated from the spleen of recipient *Rag2<sup>-/-</sup>* mice. **(D)** HSNE clustering analysis of Ctrl and

*Ebi3*<sup>-/-</sup> CD4<sup>+</sup> T cells based on ROR- $\gamma$ t, FOXP3, CD25, Ki-67, GATA3, CD103, T-bet, and GITR expression measured by FC. Heatmap comprising the clusters generated by HSNE analysis and HSNE plots depicting the expression of individual markers. **(E)** Percentages of cluster distribution in WT and *Ebi3*<sup>-/-</sup> CD4<sup>+</sup> T cells. Unpaired t test, \* *P* < .05.

**Figure S5: CD8<sup>+</sup> T cells, but not Tconv or Tregs, show major transcriptional changes in the absence of EB13.**

**(A)** Heatmap comparing the transcriptome of Ctrl and *Ebi3*<sup>-/-</sup> CD8<sup>+</sup> T cells. **(B)** Heatmaps depicting the transcriptional changes associated with translation initiation (left) and rRNA processing (right) between Ctrl and *Ebi3*<sup>-/-</sup> CD8<sup>+</sup> T cells. **(C)** Heatmap depicting the similarity of *Ebi3*<sup>-/-</sup> CD8<sup>+</sup> T cells with subsets of exhausted T cells described in [4]. **(D)** Principal component analysis (PCA) of *Ebi3*<sup>-/-</sup> CD8<sup>+</sup> T cells with the aforementioned subsets. **(E-F)** Volcano plot showing differentially expressed genes (DEG) in Ctrl and *Ebi3*<sup>-/-</sup> **(E)** Tregs and **(F)** Tconv.

**Figure S6: *Ebi3* depletion in CD8<sup>+</sup> T cells does not affect cytokine production after 3 days of activation.**

**(A)** Frequency of cells expressing the selected markers in Ctrl vs *Ebi3*<sup>-/-</sup> CD8<sup>+</sup> T cells after 3 days of activation. **(B-C)** HSNE clustering analysis of Ctrl and *Ebi3*<sup>-/-</sup> CD8<sup>+</sup> T cells based on IL-2, Ki-i67, IFN- $\gamma$ , CD44, CD39 and Granzyme B expression measured by FC at day 3 post activation. HSNE plots depicting the expression of individual markers. **(D)** Percentages of cluster distribution of Ctrl vs *Ebi3*<sup>-/-</sup> CD8<sup>+</sup> T cells after 6 days of activation. **(E)** Cytotoxicity of *Ebi3*<sup>-/-</sup> CD8<sup>+</sup> T cells in absence or presence of IL-27 against TCL1 splenocytes. **(F)** Experimental design of the 3D killing assay. Human PBMCs were isolated from four healthy donors and activated *in vitro* for 6 days in presence or absence of rhIL-27. At day 6, pulsed NALM6 cells transfected with the viability pCasper vector were added to the culture for 30h and live cell imaging was recorded. (scale bar, 50 $\mu$ m) Percentage of living target cells was calculated in the 3 conditions (activated PBMCs only, and in presence or absence of IL-27). **(G)** Bar chart showing the percentage of living target cells 10 hours after the start of the killing activity of CD8<sup>+</sup> T cells. **(H)**

Individual plots representing the kinetic of cell killing for the four donors. Unpaired t test, \*\*  $P < .01$ , \*\*\*  $P < .001$ .

**Figure S7: IL-27 does not affect human and murine CLL cells**

(A) Relative gene expression of *EBI3* in different human cell subsets in CLL patients and healthy controls. (B) Relative gene expression of *Ebi3* in different murine cell subsets in Ctrl and *E $\mu$ -TCL1* mice. (C) Viability (D) and phenotype of patient-derived CLL cells after 48h of treatment with increasing levels of IL-27. (E) Viability and (F) phenotype of *E $\mu$ -TCL1*-derived splenocytes after 48h of treatment with increasing levels of IL-27. Unpaired T test, \*  $P < .05$ , \*\*  $P < .01$ .

**Figure S8: IL-27 neutralization partially recapitulates the less immunosuppressive microenvironment observed in the transgenic mouse model.**

(A) Percentage of CD8<sup>+</sup> T among total T cells. (B-C) HSNE clustering analysis of splenic CD8<sup>+</sup> T cells from isotype- and  $\alpha$ -IL-27-treated mice based on CD62L, TIGIT, KLRG1, PD1, Ki-67, and CD44 expression measured by FC. Heatmap comprising the clusters generated by HSNE analysis and HSNE plots depicting the expression of individual markers (D) Percentages of cluster distribution between CD8<sup>+</sup> T cells derived from the spleen of isotype- or  $\alpha$ -IL-27-treated mice. (E) Percentage of CD4<sup>+</sup> T cells out of total T cells. (F) Percentage of Tconv and Tregs out of CD4<sup>+</sup> T cells. (G) Frequency of the indicated Treg populations. (H) HSNE clustering analysis and heatmap of splenic CD4<sup>+</sup> T cells from isotype- and  $\alpha$ -IL-27-treated mice based on CD62L, TIGIT, KLRG1, PD1, Ki-67, and CD44 expression measured by FC. (I) Percentages of cluster distribution between splenic CD4<sup>+</sup> T cells from isotype- or  $\alpha$ -IL-27-treated mice. Unpaired T test, \*  $P < .05$ .

**Supplemental Table 1: List of antibodies used in flow cytometry**

Antigen	Fluorochrome	Clone	Specificity	Manufacturer	Product #	Other name	RRIDs
CD103	APC	2E7	Mouse	Biolegend	121414		AB_1227502
CD11b	PE-Cy7	M1/70	Mouse/Human	Biolegend	101215		AB_312798
CD11c	APC-V770	1B29	Mouse	Miltenyi	130-107-461		AB_2783921
CD134	APC	REA625	Mouse	Miltenyi	130-109-742	OX40	AB_2654942
CD152	PE	UC10-4B9	Mouse	Biolegend	106305	CTLA4	AB_313255
CD19	FITC	eBio1D3	Mouse	ThermoFisher	11-0193-86		AB_657665
CD19	PE-Cy7	eBio1D3	Mouse	ThermoFisher	25-0193-82		AB_657663
CD19	APC	6D5	Mouse	Biolegend	115512		AB_313647
CD19	Biotin	6D5	Mouse	Miltenyi	130-101-951		AB_2801732
CD25	BV421	PC61	Mouse	Biolegend	102043	IL-2R $\alpha$	AB_11203373
CD25	FITC	REA568	Mouse	Miltenyi	130-108-999		AB_2656653
CD25	BV421	PC61	Mouse	Biolegend	102043		AB_2562611
CD279	BV510	29F.1A12	Mouse	Biolegend	135241	PD-1	AB_2715761
CD3	PerCP	1B8	Mouse	Biolegend	100326		AB_893317
CD3	Biotin	1B3	Mouse	Miltenyi	130-109-835		AB_2751822
CD357	PerCP/Cy5.5	DTA-1	Mouse	Biolegend	126316	GITR	AB_2563384
CD39	PE-Cy7	Duha59	Mouse	Biolegend	143805		AB_2563393
CD4	APC-Fire 750	1B13	Mouse	Biolegend	100568		AB_2629699
CD4	APC-Cy7	RM4-5	Mouse	Biolegend	100526		AB_312727
CD44	FITC	IM7	Mouse	Biolegend	103022		AB_312957
CD44	AF700	IM7	Mouse	Biolegend	103026		AB_493713
CD44	PE	IM7	Mouse	Biolegend	103008		AB_312959
CD44	APC	IM7	Mouse/Human	Biolegend	103012		AB_312963
CD5	PE	53-7.3	Mouse	Biolegend	100608		AB_312737
CD5	APC	53-7.3	Mouse	Biolegend	100626		AB_2563929
CD62L	PE-Cy7	MEL-14	Mouse	Biolegend	104418		AB_313103
CD69	AF700	FN50	Human	Biolegend	310922		AB_493775
CD73	APC	TY/11.8	Mouse	Biolegend	127209		AB_11218786
CD8	BV650	1B21	Mouse	Biolegend	100742		AB_2563056
F4/80	BV421	BM8	Mouse	Biolegend	123137		AB_11203717
Foxp3	APC	REA788	Mouse	Miltenyi	130-111-601		AB_2651766
Foxp3	BV488	MF-14	Mouse	Biolegend	126406		AB_1089113
GATA3	BV421	16E10A23	Mouse/Human	Biolegend	653814		AB_2563221
Granzyme B	PE	QA16A02	Mouse/Human	Biolegend	372208		AB_2687032
HLA-A,B,C	PE-Cy7	W6/32	Human	Biolegend	311430		AB_2561617
IFN $\gamma$	BV711	XMG1.2	Mouse	Biolegend	505836		AB_2650928
IL-10	BV421	JES3-9D7	Human	Biolegend	501421		AB_10896947

<b>IL17A</b>	PE	TC11-18H10	Mouse	Miltenyi	130-102-344		AB_2660786
<b>IL2</b>	PE-Cy7	JES6-5H4	Mouse	Biolegend	503832		AB_2561750
<b>Ki-67</b>	BV421	16A8	Mouse	Biolegend	652411		AB_2562663
<b>Ki-67</b>	APC	16A8	Mouse	Biolegend	652406		AB_2561930
<b>Ki-67</b>	BV421	16A8	Mouse	Biolegend	652411		AB_2562663
<b>KLRG1</b>	BV711	2F1/KLRG1	Mouse	Biolegend	138427	MAFA	AB_2629721
<b>LAG-3</b>	BV421	C9B7W	Mouse	Biolegend	125221	CD223	AB_2572080
<b>LAG-3</b>	APC	7H2C65	Human	Biolegend	369211	CD223	AB_2728372
<b>Ly6c</b>	PE	1G7.G10	Mouse	Miltenyi	130-102-391		AB_2857638
<b>Ly6G</b>	Biotin	REA526	Mouse	Miltenyi	130-107-911	Gr-1	AB_2727584
<b>MHC-DR</b>	APC	L243	Human	Biolegend	980406		AB_2650655
<b>MHC-I</b>	PE	28-8-6	Mouse	Biolegend	114607		AB_313598
<b>MHC-II</b>	BV650	M5/114.15.2	Mouse	Biolegend	107641	I-A/I-E	AB_2565975
<b>NK1.1</b>	Biotin	PK136	Mouse	Miltenyi	130-101-888	CD161	AB_2727573
<b>PD-L1</b>	APC	29E2A3	Human	Biolegend	329707	CD274	AB_940358
<b>PD-L1</b>	APC	29E2A3	Human	Biolegend	329707	CD274	AB_940358
<b>RORg (t)</b>	PE	B2D	Mouse	eBioscience	2054914		AB_10805392
<b>Tbet</b>	PE-Cy7	4B10	Mouse/Human	Biolegend	644823		AB_2561760
<b>TGF-β</b>	PerCP/Cy5.5	TW7-16B4	Mouse	Biolegend	141409		AB_2561591
<b>TIGIT</b>	PE	GIGD7	Mouse	eBiosciences	12-950182		AB_11042152
<b>TNFα</b>	APC	MP6-XT22	Mouse	Biolegend	506308		AB_315429
<b>TOX</b>	PE	TXRX10	Mouse	eBioscience	12-6502-82		AB_10855034

<b>eBioscience™ Fixable Viability Dye eFluor® 506</b>		ThermoFisher	65-0866-18
<b>Zombie Green™ Fixable Viability Kit</b>		Biolegend	423111
<b>Zombie RED™ Fixable Viability Kit</b>		Biolegend	423109
<b>Zombie UV™ Fixable Viability Kit</b>		Biolegend	423108
<b>Zombie NIR™ Fixable Viability Kit</b>		Biolegend	423106

**Figure S1**

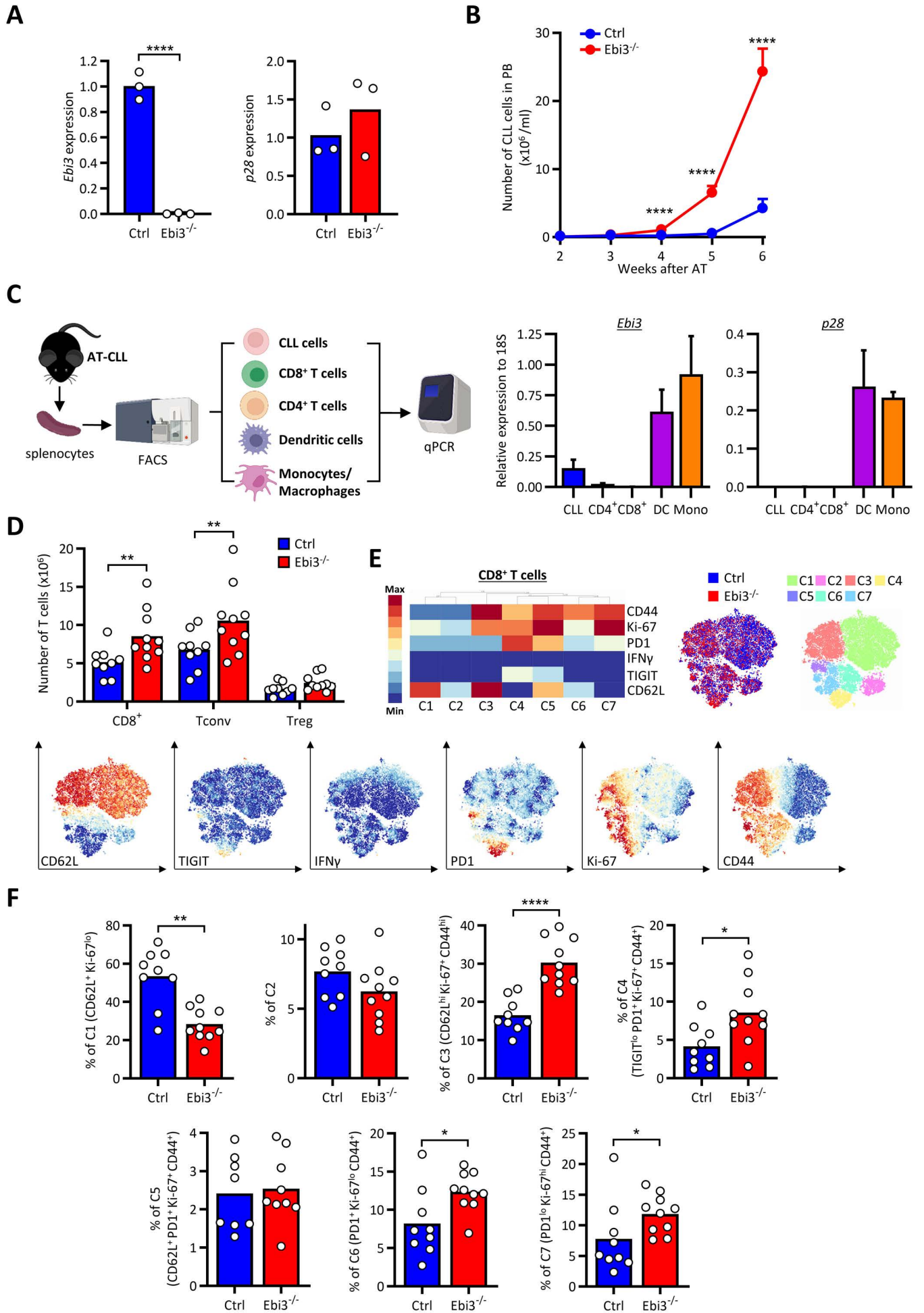
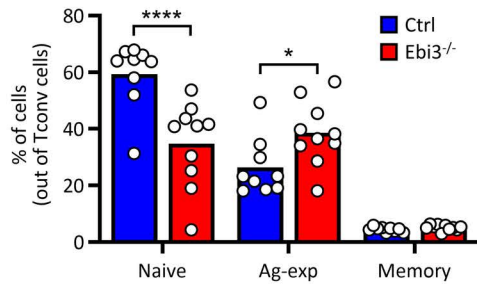
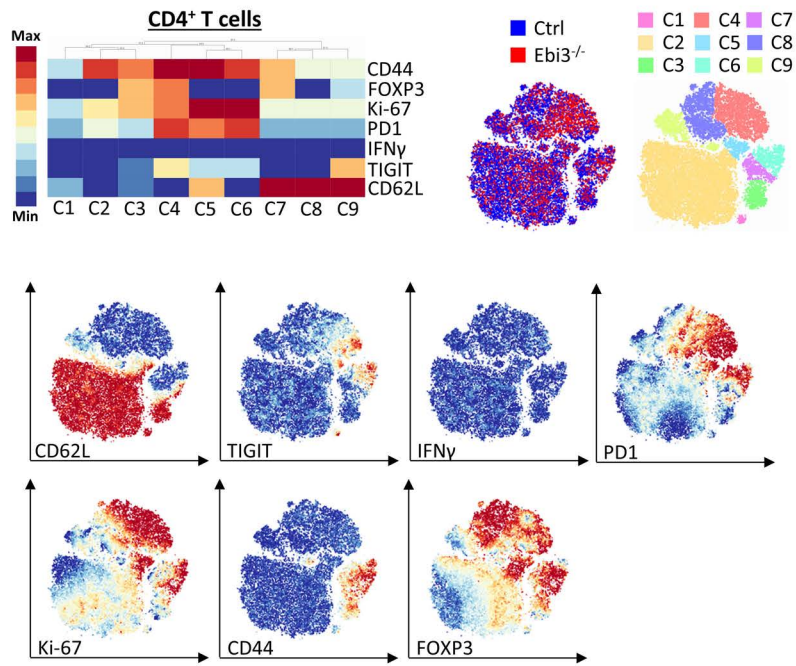


**Figure S1**

**G**



**H**



**I**

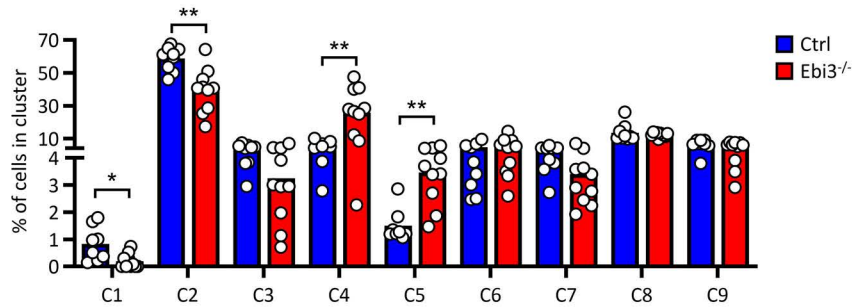


**Figure S2**

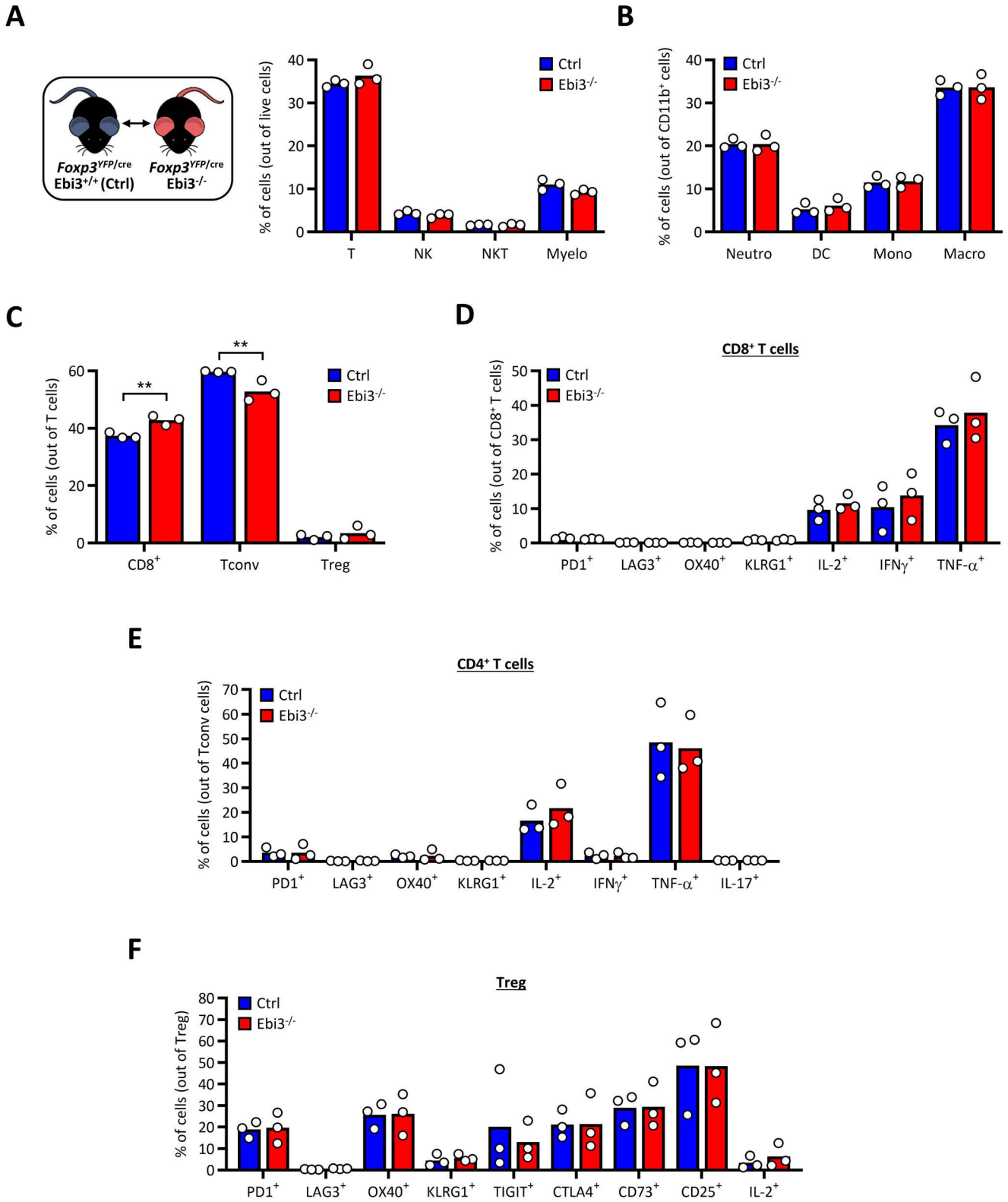


**Figure S3**

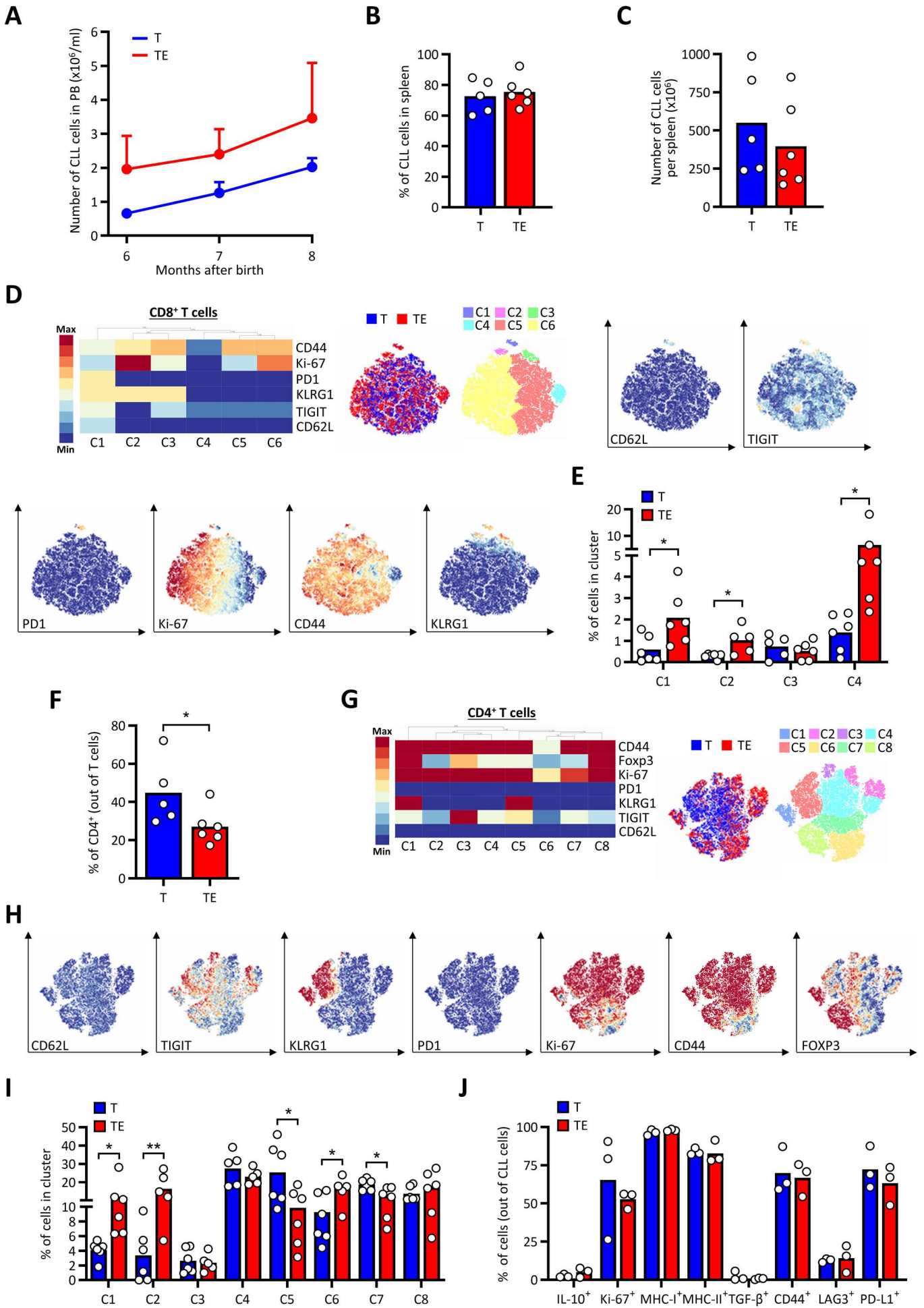


**Figure S4**

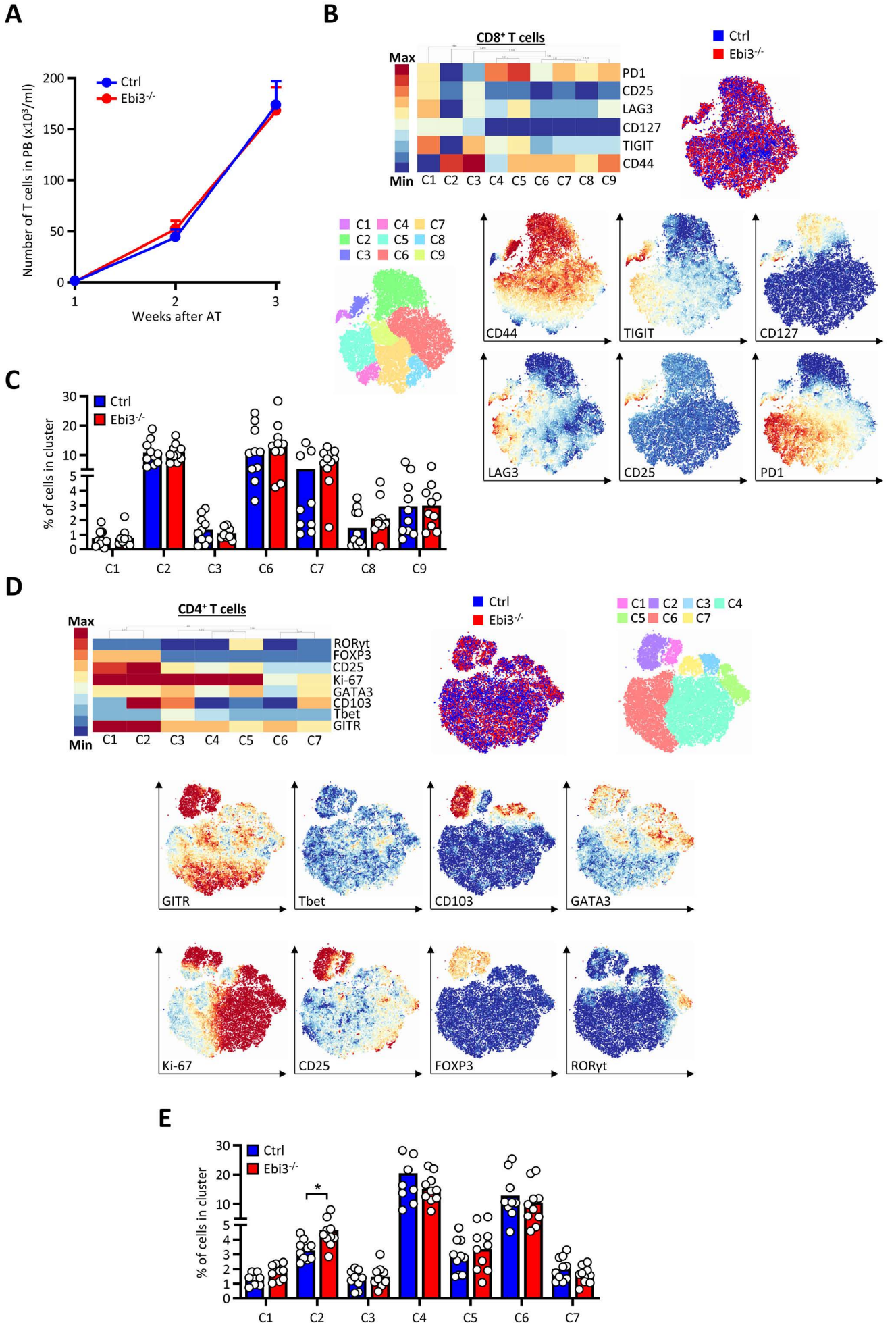


**Figure S5**

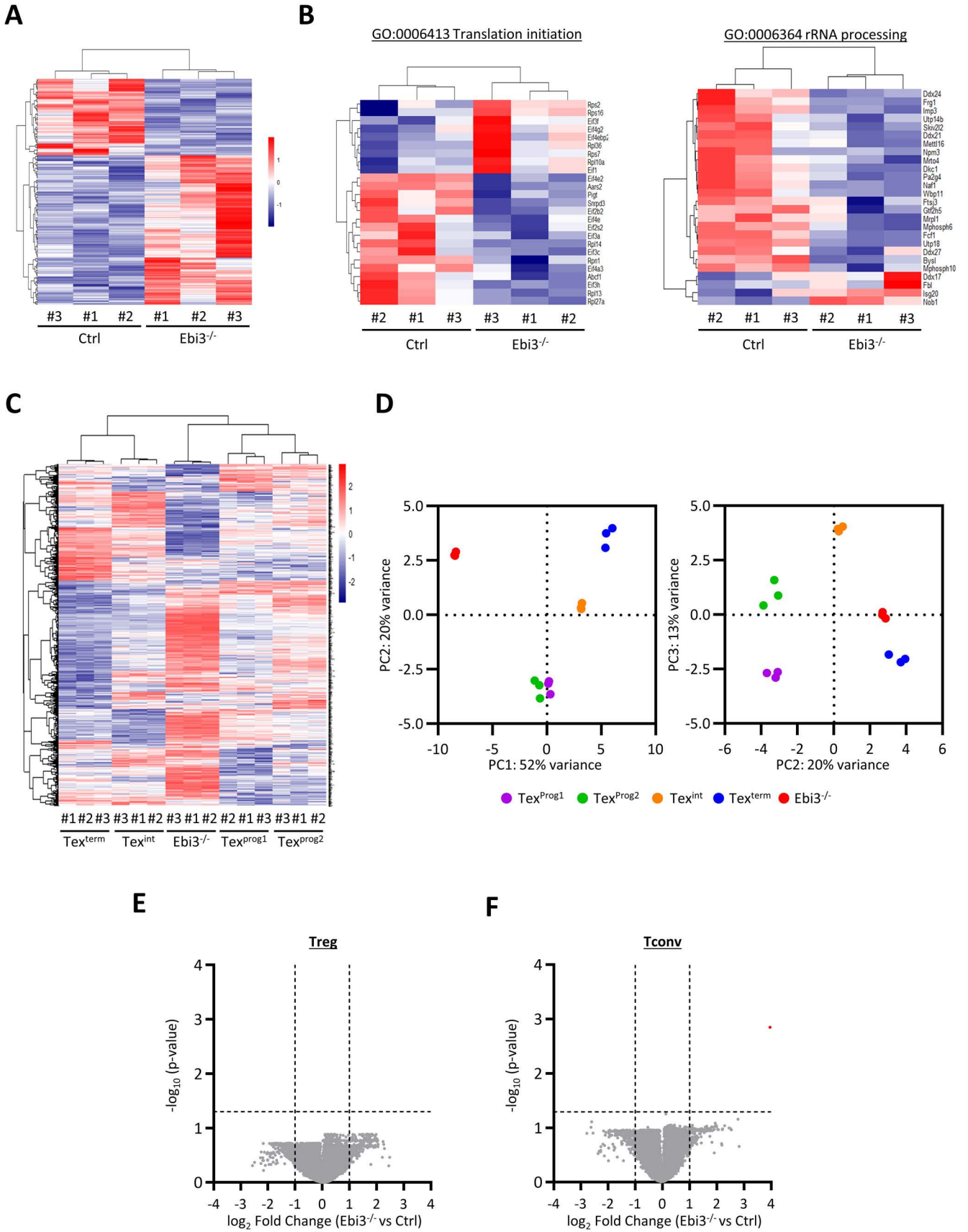


**Figure S6**

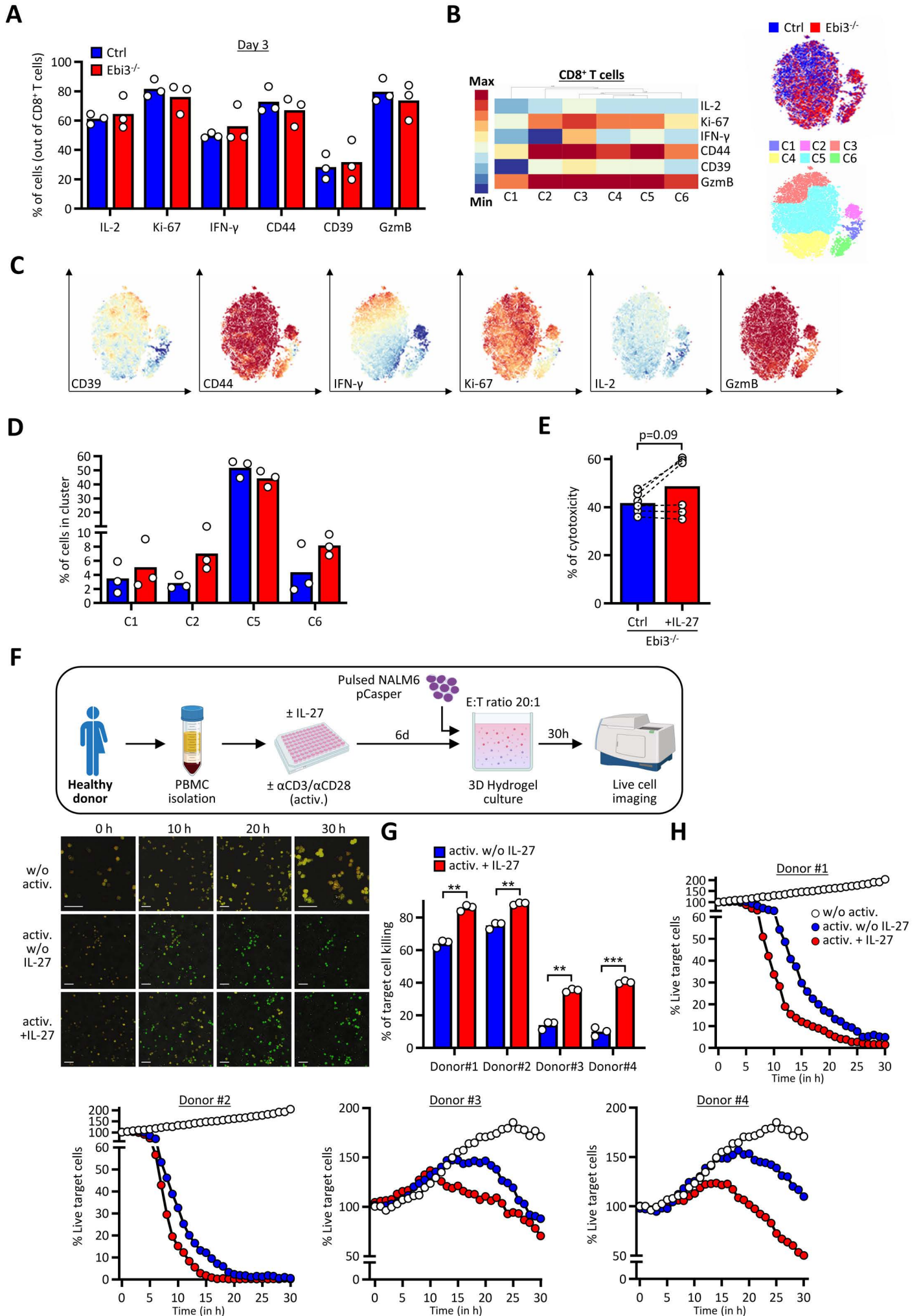
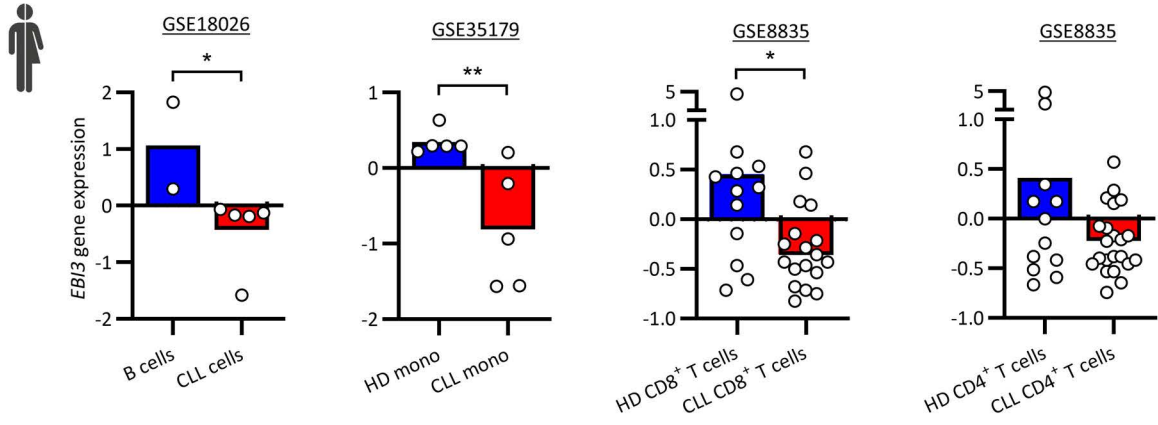
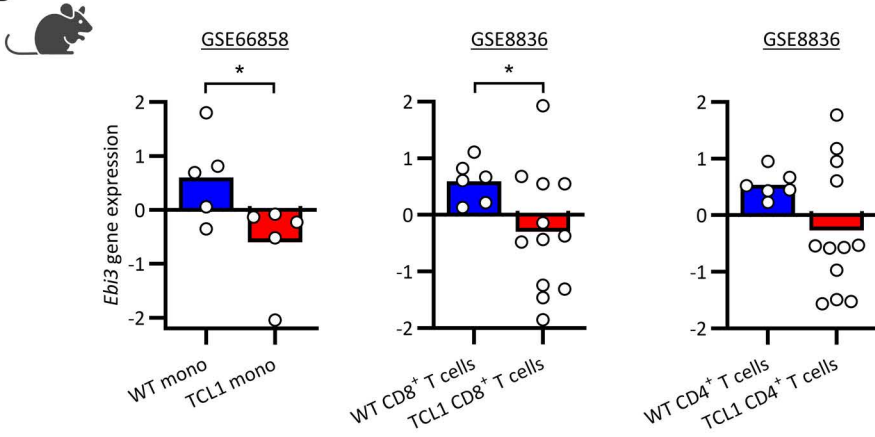


Figure S7

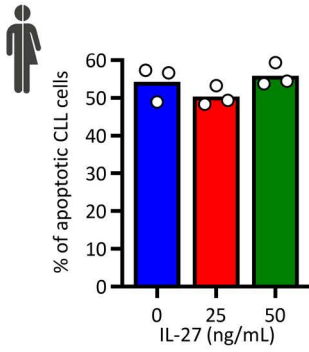
A



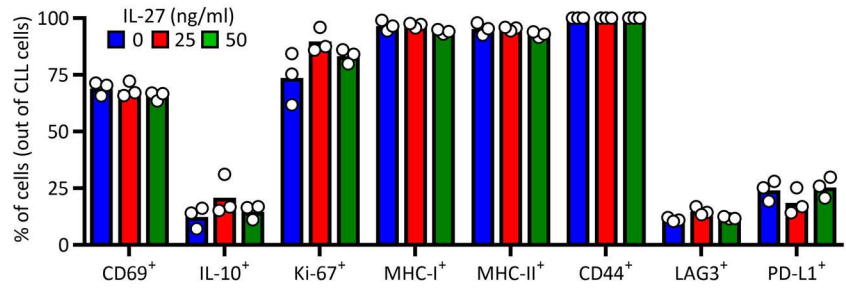
B



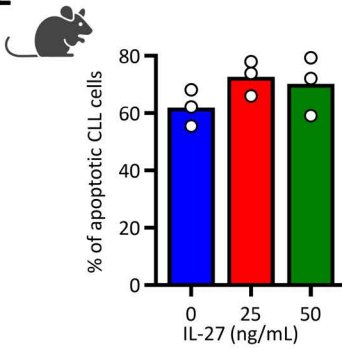
C



D



E



F

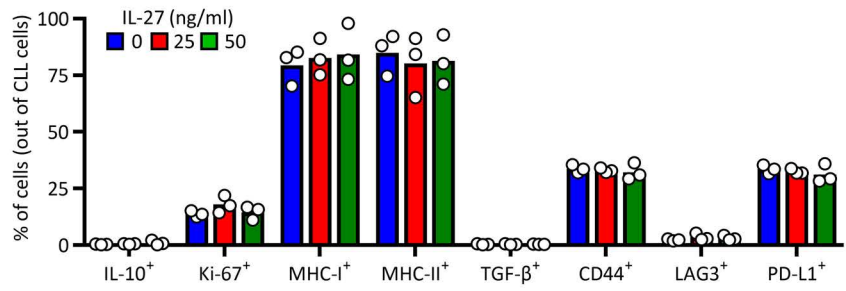


**Figure S8**

